Published in final edited form as:
Int J Non Linear Mech. 2012 June 1; 47(5): 506–520. doi:10.1016/j.ijnonlinmec.2011.09.025.

Modeling and numerical simulation of blood flow using the Theory of Interacting Continua

Mehrdad Massoudi[1], **Jeongho Kim**[2], and **James F. Antaki**[2]

[1]U. S. Department of Energy, National Energy Technology Laboratory (NETL), P. O. Box 10940 Pittsburgh, PA, 15236 USA

[2]Department of Biomedical Engineering, Carnegie Mellon University, Pittsburgh, PA, 15213 USA

Abstract

In this paper we use a modified form of the mixture theory developed by Massoudi and Rajagopal to study the blood flow in a simple geometry, namely flow between two plates. The blood is assumed to behave as a two-component mixture comprised of plasma and red blood cells (RBCs). The plasma is assumed to behave as a viscous fluid whereas the RBCs are given a granular-like structure where the viscosity also depends on the shear-rate.

Keywords

Mixture Theory; blood; continuum mechanics; shear-thinning; two-phase flows

1. Introduction

The safety and efficiency of blood-wetted medical devices are closely tied to the physical and biological processes governing the transport of blood. This has led to research in blood rheology, trauma, and thrombosis. Despite these efforts, a fundamental understanding of device-induced blood trauma remains incomplete. Due to a lack of predictive mathematical tools, the primary means to study the blood trauma is the costly method of experimental trial-and-error. It is therefore necessary to develop more accurate models for blood trauma and hemorheology, especially for applications in the blood-wetted devices.

It is known that in large vessels (whole) blood behaves as a Navier-Stokes (Newtonian) fluid (see Fung (1993, Chapter 3) (Fung 1993)); however, in a vessel whose characteristic dimension (diameter for example) is about the same size as the characteristic size of blood cells, blood behaves as a non-linear fluid, exhibiting shear-thinning and stress relaxation. Thurston (Thurston 1972; Thurston 1973) pointed out the viscoelastic behavior of blood while stating that the stress relaxation is more significant for cases where the shear rate is low. The micro-scale flow and deformation of blood have been studied for many years. Early *in vitro* investigations in rotational viscometers or small glass tubes revealed the characteristic rheological properties such as the reduction in the blood apparent viscosity (Chien, Usami et al. 1966), Fahraeus effect (Fahraeus 1929) and Fahraeus-Lindqvist effect (Fahraeus and Lindqvist 1931), revealing the manifestation nonhomogeneity of blood in

MASSOUDI@NETL.DOE.GOV.

microcirculation. Similarly, the microscopic phenomenon responsible for shear-thinning is found to be the flexibility and alignment of red blood cells (RBCs) at high shear, and shear-thickening due to the aggregation of cells at low shear (as shown in Figure 21 of (Galdi, Rannacher et al. 2008)). A further result of the multi-component character of blood is the plasma-skimming phenomenon, whereby the hematocrit in branches of blood vessels with size below 300 micron is reduced due to a phase separation and deficit of RBCs near the wall of the parent vessel (Carr and Wickham 1990). Consideration of the cellular component also involves cell-cell interaction (Goldsmith, Takamura et al. 1983) and cell-surface interaction (Goldsmith 1971). The migration toward the centerline and the rotation of the RBCs are believed to increase the platelet diffusivity and expel the platelet to the near wall region, platelet margination (Aarts, Vandenbroek et al. 1988).

Microscopic models of blood flow (Bagchi 2007) that account for cell-scale lift and drag forces, collisions, deformation, etc. have the potential to replicate some of the phenomena causing the non-homogeneous distribution of RBCs and platelets. However, for most problems of practical value, it is prohibitive to consider the three-dimensional dynamic interactions of individual blood cells – which may amount to several thousand to millions. This has motivated the pursuit of meso-scale multi-phase (or multi-component) models as a reasonable compromise between specificity and practicality. Motivated primarily by the plasma-skimming phenomenon (Carr and Wickham 1990), investigators have developed four classes of multi-phase models for blood: *edge-core* (Sharan and Popel 2001), *averaging* (Jung and Hassanein 2008), *immersed particle* (Hyun, Kleinstreuer et al. 2000), and *effective medium* approach (Pal 2003).

In this paper we advocate using Mixture Theory or the theory of Interacting Continua, to propose a two-component model for blood. The large numbers of articles published concerning multi-component flows typically employ one of the two continuum theories developed to describe such situations: Mixture Theory (or the theory of interacting continua) (Rajagopal and Tao (1995) (Rajagopal and Tao 1995)) or Averaging Method(s) (Ishii 1975). Both approaches are based on the underlying assumption that each component may be mathematically described as a continuum. The Averaging method directly modifies the classical transport equations to account for the discontinuities or 'jump' conditions at moving boundaries between the components (cf. Anderson and Jackson (Anderson and Jackson 1967), Drew and Segal (Drew and Segel 1971), Gidaspow (Gidaspow 1994), Jung et al (Jung, Hassanein et al. 2006; Jung and Hassanein 2008)). Although the two methods seem similar, the way they approach the formulation of constitutive models are very different. In fact, as shown in Massoudi (2002) (Massoudi 2002), many of the interaction models used by researchers in the Averaging community are not frame-indifferent, thus violating basic principles in physics. Other differences between the two approaches are explained in Johnson et al (1991a, b) (Johnson, Massoudi et al. 1991; Johnson, Massoudi et al. 1991), and Massoudi et al (Massoudi, Rajagopal et al. 1992; Massoudi, Rajagopal et al. 1999).

For example, in order to better understand atherosclerosis, Jung et al in 2008 (Jung and Hassanein 2008) used the averaging approach to simulate a three-component blood flow (RBC-WBC-plasma) in the right coronary artery using a commercial CFD package software (ANSYS FLUENT, Canonsburg, PA), but there are several limitations in that study. For example, the employed drag model is valid only for solid spherical particles or for fluid particles that are sufficiently small, whereas RBCs in flows of interest are usually non-spherical and not negligible in size . Further, the 3-dimensional Eulerian-Eulerian code used is not appropriate for such dense concentration of RBCs (45% hematocrit) as studied. Also, Jung's definition of the relative blood mixture viscosity is not very clear. Massoudi (Massoudi 2008) has discussed this issue in more detail. Furthermore, many of constitutive

models used in the averaging methods in general and specifically in Jung et al (Jung, Hassanein et al. 2006) are not frame-indifferent, for example, the virtual mass term and the shear lift force violate the principle of frame-indifference [For more details see Massoudi (Massoudi 2002).

In Section 2 of this paper, we provide a brief review of Mixture Theory, and then discuss certain issues in constitutive modeling of blood. In the present formulation we assume blood to form a mixture consisting of RBCs suspended in plasma, while ignoring the platelets, the white blood cells (WBCs) and the proteins in the sample. No biochemical effects or interconversion of mass are considered in this model. The volume fraction (or the concentration of the RBCs) is treated as a field variable. We further assume that the plasma behaves as a linearly viscous fluid and the RBCs as an anisotropic non-linear density-gradient-type fluid (see Massoudi and Antaki (2008) (Massoudi and Antaki 2008)). In Section 3, we discuss the constitutive modeling of the stress tensors and the interaction forces. In Section 4, we study and solve numerically the equations of motion for the fully developed flow of such a mixture between two horizontal flat plates. Finally, in Section 5, we present numerical solutions for a few cases.

2. A brief review of Mixture Theory

Mixture Theory, or the Theory of Interacting Continua, traces its origins to the work of Fick in 1855 (see (Rajagopal 2007)) and was first presented within the framework of continuum mechanics by Truesdell (Truesdell 1957). It is a means of generalizing the equations and principles of the mechanics of a single continuum to include any number of superimposed continua. More detailed information, including an account of the historical development, is available in the articles by Atkin and Craine (Atkin and Craine 1976; Atkin and Craine 1976), Bowen (Bowen 1976), Bedford and Drumheller (Bedford and Drumheller 1983), and in the books by Truesdell (Truesdell 1984), Samohyl (Samohyl 1987), and Rajagopal and Tao (Rajagopal and Tao 1995). Mixture Theory has also been used in a variety of biomechanics applications (Mow, Kuei et al. 1980; Mow, Holmes et al. 1984; Lai, Hou et al. 1991; Gu, Lai et al. 1998; Klisch and Lotz 2000; Kuhn and Hauger 2000; Tao, Humphrey et al. 2001; Humphrey and Rajagopal 2002; Garikipati, Arruda et al. 2004; Araujo and Mcelwain 2005; Axtell, Park et al. 2005; Araujo and McElwain 2006; Ateshian, Likhitpanichicul et al. 2006; Lemon, King et al. 2006; Ateshian 2007).

Let $\mathbf{X}_1$ and $\mathbf{X}_2$ denote the positions of particles of S_1 and S_2 in the reference configuration. The motion of the constituents is represented by the mappings:

$$\mathbf{x}_1=\chi_1(\mathbf{X}_1, t), \text{ and } \mathbf{x}_2=\chi_2(\mathbf{X}_2, t). \tag{1}$$

These motions are assumed to be one-to-one, continuous, and invertible. The kinematical quantities associated with these motions are:

$$\begin{aligned}&\mathbf{v}_1=\frac{d_1\chi_1}{dt};\ \mathbf{v}_2=\frac{d_2\chi_2}{dt},\ \mathbf{a}_1=\frac{d_1\mathbf{v}_1}{dt},\ \mathbf{a}_2=\frac{d_2\mathbf{v}_2}{dt},\ \mathbf{L}_1=\frac{\partial\mathbf{v}_1}{\partial\mathbf{x}_1},\ \mathbf{L}_2=\frac{\partial\mathbf{v}_2}{\partial\mathbf{x}_2},\\ &\mathbf{W}_1=\tfrac{1}{2}(\mathbf{L}_1-\mathbf{L}_1^T),\ \mathbf{W}_2=\tfrac{1}{2}(\mathbf{L}_2-\mathbf{L}_2^T),\ \mathbf{D}_1=\tfrac{1}{2}(\mathbf{L}_1+\mathbf{L}_1^T),\ \mathbf{D}_2=\tfrac{1}{2}(\mathbf{L}_2+\mathbf{L}_2^T),\end{aligned} \tag{2}$$

where $\mathbf{v}$ denotes velocity, $\mathbf{a}$ is acceleration, $\mathbf{L}$ is the velocity gradient, $\mathbf{D}$ denotes the symmetric part of the velocity gradient, and $\mathbf{W}$ is the spin tensor. d_1/dt denotes differentiation with respect to t, holding $\mathbf{X}_1$ fixed, and d_2/dt denotes the same operation holding $\mathbf{X}_2$ fixed. Also, ρ_1 and ρ_2 are the bulk densities of the mixture components given by:

$$\rho_1=\gamma\rho_{10},\ \rho_2=\phi\rho_{20}, \tag{3}$$

where ρ_{10} is the pure density of the component 1, ρ_{20} is the pure density of component 2, γ is the volume fraction of the component 1, and φ is the volume fraction of component 2. For a saturated mixture $\gamma = 1 - \varphi$. The mixture density, ρ_m and the mean velocity $\mathbf{v_m}$ of the mixture are defined by:

$$\rho_m = \rho_1 + \rho_2, \quad \rho_m \mathbf{v}_m = \rho_1 \mathbf{v}_1 + \rho_2 \mathbf{v}_2. \tag{4)a,b}$$

Assuming no interconversion of mass between the two constituents, conservation of mass for the two components are:

$$\frac{\partial \rho_1}{\partial t} + \mathrm{div}(\rho_1 \mathbf{v}_1) = 0, \quad \frac{\partial \rho_2}{\partial t} + \mathrm{div}(\rho_2 \mathbf{v}_2) = 0. \tag{5)a,b}$$

If $\mathbf{T}_1$ and $\mathbf{T}_2$ denote the partial stress tensors of the two components, then the equations for the balance of linear momentum are given by:

$$\rho_1 \frac{d_1 \mathbf{v}_1}{dt} = \mathrm{div}\, \mathbf{T}_1 + \rho_1 \mathbf{b}_1 + \mathbf{f}_1, \quad \rho_2 \frac{d_2 \mathbf{v}_2}{dt} = \mathrm{div}\, \mathbf{T}_2 + \rho_2 \mathbf{b}_2 - \mathbf{f}_1, \tag{6)a,b}$$

where $\mathbf{b}$ represents the body force, and $\mathbf{f}_I$ represents the interaction forces (exchange of momentum) between the components. The balance of moment of momentum implies that:

$$\mathbf{T}_1 + \mathbf{T}_2 = \mathbf{T}_1^{\mathbf{T}} + \mathbf{T}_2^{\mathbf{T}} \tag{7}$$

which implies that the total stress tensor is symmetric; however, the partial stresses need not be symmetric. With these equations as the basis, in order to solve any two-component flow problem, one needs to specify or derive the constitutive relations for the interaction forces [see Massoudi (2002, 2003) (Massoudi 2002; Massoudi 2003)] and the stress tensors. This is called the 'closure' problem in the two-phase community. In the next section, we discuss the constitutive relations used in our study.

3. Constitutive equations

Deriving constitutive relations for the stress tensors and the interaction forces are among the outstanding issues of research in multicomponent flows. In general, the constitutive expressions for $\mathbf{T}_1$ and $\mathbf{T}_2$ depend on the kinematical quantities associated with both the constituents. However, it can be assumed that $\mathbf{T}_1$ and $\mathbf{T}_2$ depend only on the kinematical quantities associated with the plasma (component 1) and the RBCs (component 2), respectively (sometimes called the principle of component (phase) separation, see Adkins (Adkins 1963; Adkins 1963)).

Here we provide a brief description of a mixture theory formulation proposed by Massoudi and Rajagopal [M-R]. In this approach, we consider a mixture of an incompressible fluid infused with solid particles, wherein the principles of mechanics of granular materials are used to describe the behavior of particles. This model has been used and discussed in Massoudi (Massoudi 1986; Massoudi 1988; Massoudi 2001; Massoudi 2002; Massoudi 2003; Massoudi 2003; Massoudi 2007; Massoudi 2008), Johnson et al, (Johnson, Massoudi et al. 1991; Johnson, Massoudi et al. 1991), Rajagopal, et al (Rajagopal, Troy et al. 1992; Rajagopal, Massoudi et al. 1994), Massoudi et al (Massoudi, Rajagopal et al. 1999), Massoudi and Johnson (Massoudi and Johnson 2000), and Massoudi and Rao (Massoudi and Rao 2001), Ravindran et al (Ravindran, Anand et al. 2004), Massoudi (Massoudi 2008; Massoudi 2010). We need to mention that alternatively blood can be viewed as a suspension where it can be modeled using the techniques of non-Newtonian fluid mechanics. We,

however, assume that blood is a two-component mixture, composed of the red blood cells (RBCs) suspended in a (platelet rich) plasma.

In the following description, the plasma in the mixture will be represented by S_1 and the RBCs by S_2. We also assume that φ represents the concentration of the RBCs, also commonly referred to as hematocrit (Ht). Now, ρ_1 and ρ_2 are the bulk densities of the mixture components given by: $\rho_1 = \gamma\rho_P$, $\rho_2 = \varphi\rho_{RBC}$, where ρ_P is the density of the plasma, ρ_{RBC} is the density of the RBCs, φ is the volume fraction of the RBCs, and γ is the volume fraction of the plasma. Once the individual stress tensors are derived (or proposed), a mixture stress tensor can be defined as $\mathbf{T}_m = \mathbf{T}_1 + \mathbf{T}_2$, where $\mathbf{T}_1 = (\mathbf{1} - \boldsymbol{\varphi})\mathbf{T}_P$ and $\mathbf{T}_2 = \mathbf{T}_R$, so that the mixture stress tensor reduces to that of plasma as $\varphi \rightarrow 0$ and to that of a RBCs as $\gamma \rightarrow 0$. Note that $\mathbf{T}_2$ may also be written as $\mathbf{T}_2 = \phi\hat{\mathbf{T}}_R$, where $\hat{\mathbf{T}}_R$ may be thought of as representing the stress tensor in a reference configuration. Kesmarky et al. (Kesmarky, Kenyeres et al. 2008) show that plasma behaves like a Newtonian fluid and for the range of shear rates studied there is no significant departure from linearity. Accordingly, the constitutive relation for plasma is assumed to be

$$\mathbf{T}_1=[-p(\rho_1)+\lambda_1(\rho_1)\mathrm{tr}\,\mathbf{D}_1]\mathbf{I}+2\mu_1(\rho_1)\mathbf{D}_1 \tag{8}$$

where p is the fluid pressure, $\mathbf{I}$ is the identity tensor, μ_1 is the viscosity and $\mathbf{D}_1$ is the symmetric part of the velocity gradient of the plasma, and λ_1 is the second coefficient of viscosity. We assume that the mixture is saturated, i.e., $\gamma = 1 - \varphi$; furthermore we assume that

$$\begin{aligned} p(\rho_1)&=p(1-\phi)\\ \lambda_1(\rho_1)&=\lambda(1-\phi)\\ \mu_1(\rho_1)&=\mu(1-\phi) \end{aligned} \tag{9}$$

and thus Eqn (8) becomes:

$$\mathbf{T}_1=[-p(1-\phi)+\lambda(1-\phi)\mathrm{tr}\,\mathbf{D}_1]\mathbf{I}+2\mu(1-\phi)\mathbf{D}_1 \tag{10}$$

where p is the pressure, μ is the 'pure' viscosity, i.e., the viscosity before mixing, and λ is the 'pure' second coefficient of viscosity.

The RBCs in general should be represented as an anisotropic non-linear density-gradient-type fluid (Massoudi and Antaki 2008). In the current study, we use a simplified version of their model which was also proposed by Massoudi and Rajagopal for granular materials. According to this model, the Cauchy stress tensor $\mathbf{T}$ depends on the volume fraction φ, the gradient of φ, and the symmetric part of the velocity gradient tensor $\mathbf{D}_2$ (see Massoudi (2001) for details):

$$\mathbf{T}_2=[\beta_\circ+\beta_1\nabla\phi\bullet\nabla\phi+\beta_2\mathrm{tr}\,\mathbf{D}_2]\mathbf{I}+\beta_3\mathbf{D}_2+\beta_4\nabla\phi\otimes\nabla\phi+\beta_5\mathbf{D}_2^2 \tag{11}$$

where the dot designates the scalar product, '∇' the gradient operator, 'tr' the trace norm, and '$\otimes$' the outer product of two vectors, where $\rho_2 = \rho_s\varphi$, with ρ_s being constant, and the β's are material properties, which in general are functions of the appropriate principal invariants of $\mathbf{D}_2$. The volume fraction field $\varphi(\mathbf{x}, t)$ in this model represents the spatially dependent concentration of RBCs, which can be likened to a hematocrit field variable. That is, even though the RBCs are acknowledged to be distinct bodies with certain properties (shape, deformability, aggregability, etc.) this theory homogenizes the RBC phase by assuming that their ensemble influence on the flow is a continuous function of position (Collins 2005). The material properties $\beta_0 \ldots \beta_5$, can be construed to have the following rheological interpretation: β_0 is similar to pressure in a compressible fluid and is to be given by an

equation of state, β_2 corresponds to the second coefficient of viscosity in a compressible fluid, β_1 and β_4 are the material parameters connected with the distribution of the RBCs, β_3 is the viscosity, and β_5 is similar to the *cross-viscosity* of a Reiner-Rivlin fluid. A distinct feature of this model is its ability to predict the normal stress differences which are often related to dilatancy effects. In this paper we assume that the viscous effects (β_3) predominate over the effects of the gradient of RBC volume fraction, the second coefficient of viscosity and the normal stresses. Therefore, it is assumed as a first approximation that β_1, β_2, β_4, *and* β_5 are negligible. Thus, the stress tensor for the RBCs reduces to the structure:

$$\mathbf{T}_2=\beta_0\mathbf{I}+\beta_3\mathbf{D}_2 \tag{12}$$

where β_0 *and* β_3 are given by (Massoudi and Antaki 2008)

$$\beta_0=-p\phi \tag{13}$$

$$\beta_3(\phi)=\beta_{30}(\phi+\phi^2) \tag{14}$$

The first equation, namely $\beta_0 = -p\varphi$, which is different from that suggested by Massoudi and Rajagopal, in conjunction with Eqn (9)a, i.e., $p(\rho_1) = p(1-\varphi)$), imply that the total pressure is weighted (distributed) among the two components according to the volume fraction. This is an accepted assumption in many two-component theories, and unless there are clear experimental observations pointing otherwise, this is reasonable. Shear-thinning effects were incorporated by adopting a shear-dependent viscosity for the RBC phase, proposed by Yeleswarapu et al (Yeleswarapu, Kameneva et al. 1998), provided . in equation 15. The three characteristic constants μ_∞ μ_0, and κ are determined by a nonlinear regression analysis. It was indicated that this viscosity function has the least error over the widest range of shear rates when compared to other popular viscosity models. In addition, this viscosity model is able to represent the plateau viscosity at very low shear rates:

$$\beta_{30}=\mu_\infty+(\mu_0-\mu_\infty)\frac{1+\ln(1+\kappa\dot{\gamma})}{1+\kappa\dot{\gamma}} \tag{15}$$

where $\dot{\gamma}=\left[2\,\mathrm{tr}\,(\mathbf{D}_2^2)\right]^{1/2}$ is the proper norm (generalized shear rate), μ_0 is the viscosity under zero shear rate, μ_∞, is an asymptotic viscosity (for infinite shear rate), and κ is a material parameter describing the character of shear thinning. Thus,

$$\beta_3(\phi)=\left[\mu_\infty+(\mu_0-\mu_\infty)\frac{1+\ln(1+\kappa\dot{\gamma})}{1+\kappa\dot{\gamma}}\right](\phi+\phi^2) \tag{16}$$

The parameters above are theoretically associated with a homogeneous continuum comprised entirely of RBCs. This is however infeasible to test experimentally; therefore, the best practical approximation is to extrapolate from a very high concentration of RBCs for which blood continues to flow. In the present case, the seminal experimental data of Chien et al. (Chien, Usami et al. 1966) for a 90% Ht suspension of (canine) RBCs were used. (See Figure 1.)

We now turn our attention to the interaction forces which are a critical component of the Mixture Theory. Although these forces are difficult to measure explicitly, arguments from multiphase flows (Massoudi 2002; Massoudi 2003) dictate that they are generally a function of the fluid pressure gradient, density gradients, relative velocity, relative acceleration,

magnitude of the rate of the deformation tensor of the fluid, spinning motion as well as the translation of particles (Faxen's force), tendency of the particles to move toward the region of higher velocity gradients (Magnus force), history of the particle motion (Bassett force), temperature gradient and other secondary effects. If the flow is steady, the virtual mass effects can be neglected. In the absence of experimental data, various functions have been proposed by different researchers based on mathematical arguments, such as the generalization of physics of single-particles. Order-of-magnitude analysis suggests that, in most applications, the spin lift is negligible compared to the shear lift (Johnson, Massoudi et al. 1990). For the interaction forces we use a simplified version of a model proposed by Johnson et al (19991a, b) where

$$\begin{aligned}\mathbf{F}_1 = & A_1 \operatorname{grad} \phi + A_2 \phi (1+6.55\phi)(\mathbf{v}_2 - \mathbf{v}_1) \\ & + A_3 \phi (2 \operatorname{tr} \mathbf{D}_1^2)^{-1/4} \mathbf{D}_1 (\mathbf{v}_2 - \mathbf{v}_1)\end{aligned} \tag{17}$$

Where the terms on the right had side refer to diffusion, drag, and shear lift forces, respectively. Appropriate coefficients for specific interaction forces (e.g. drag force, lift force, etc) are derived from several sources. The drag coefficients and lift coefficients were directly adapted from literature (Johnson, Massoudi et al. 1990). As a first approximation, we assume A_1 to be constant. Müller's (1968) work indicates that a term of the form $A_1 \operatorname{grad} \varphi$ must be included in the interactions in order to get well-posed problems. Within the framework of mixture theory developed here, we cannot directly account for particle size, or different particle sizes, or particle shape, or surface roughness, or … However, since the coefficients in this equation are determined either by performing simple experiments on an assembly of known size and known shape particles, or by extrapolating and extending the results of a single particle, material or geometrical properties can enter in the constitutive relation through these coefficients. Therefore, we have, for example, [cf. Johnson et al. (1990) for details]:

$$A_2 = \frac{9}{2} \frac{\mu_f}{a^2}, \quad A_3 = \frac{3(6.46)}{4\pi} \frac{\rho_f^{1/2} \mu_f^{1/2}}{a} \tag{18a,b}$$

where 'a' is the particle radius. The actual form for the force due to density gradients [see Muller (1977)] multiplied by A_1 should include the terms ($\alpha_1 \operatorname{grad} \rho_1 + \alpha_2 \operatorname{grad} \rho_2$) where α_1 and α_2 are constants. If we assume that the system is a saturated mixture with incompressible components, this expression simplifies to $A_1 \operatorname{grad} \varphi$, where $A_1 = \alpha_2 - \alpha_1$.

Finally, in our approach no couple stresses are allowed. Nevertheless, in general, due to the higher order gradients of the volume fraction, it is necessary to provide additional boundary conditions [see Massoudi (2007) for a discussion of boundary conditions]. For most practical applications, these can be satisfied by certain symmetry conditions; in certain cases the values of the unknowns or their derivatives have to be specified as surface conditions at the solid walls or at the free surface.

In the next section we derive and present the dimensionless forms of the governing equations. To gain further insight into the nature and influence of the various terms in these equations, especially the constitutive parameters, we will numerically solve the simplified equations for the fully developed flow of blood, modeled as a two-component mixture (the plasma and the RBCs), between two long horizontal plates.

4. Flow between two flat plates

Substituting Eqns (10) and (17) in (6) a we obtain the dimensionless forms of the two momentum equations in their expanded forms. These are, for the plasma (component 1)

$$\begin{aligned}&(1-\phi)\rho_f\left[\frac{\partial \mathbf{V}_1}{\partial \tau}+(\text{grad}\,\mathbf{V}_1)\mathbf{V}_1\right]=(\text{grad}\,\phi)\text{P}-(1-\phi)\text{grad P}\\&+\Lambda[(-\text{grad}\,\phi)\text{div}\,\mathbf{V}_1+(1-\phi)\text{grad}\,(\text{div}\,\mathbf{V}_1)]+(1-\phi)(\text{grad}\,\Lambda)\text{div}\,\mathbf{V}_1\\&+\frac{2}{\text{Re}}[(-\text{grad}\,\phi)\mathbf{D}_1+(1-\phi)\text{div}\,\mathbf{D}_1]\\&+\frac{\rho_f}{\text{Fr}}(1-\phi)\mathbf{b}_1+C_1\text{grad}\,\phi+C_2F(\phi)(\mathbf{V}_2-\mathbf{V}_1)+C_3\phi(2\,\text{tr}\,\mathbf{D}_1^2)^{-1/4}\mathbf{D}_1(\mathbf{V}_2-\mathbf{V}_1)\end{aligned}\tag{19}$$

and for the RBCs (component 2):

$$\begin{aligned}&\phi\rho_s\left[\frac{\partial \mathbf{V}_2}{\partial \tau}+(\text{grad}\,\mathbf{V}_2)\mathbf{V}_2\right]=-(\text{grad}\,\phi)\text{P}-\phi\,\text{grad P}\\&+\left[B_{31}(\phi+\phi^2)+B_{32}(\phi+\phi^2)\prod\right]\text{div}\,\mathbf{D}_2+B_{31}\left[\text{grad}\,(\phi+\phi^2)\right]\mathbf{D}_2\\&+B_{32}\left[\text{grad}\,(\phi+\phi^2)\prod+(\phi+\phi^2)\text{grad}\,\prod\right]\mathbf{D}_2+\frac{\rho_s}{\text{Fr}}\phi\mathbf{b}_2-C_1\text{grad}\,\phi-C_2F(\phi)(\mathbf{V}_2-\mathbf{V}_1)\\&-C_3\phi(2\,\text{tr}\,\mathbf{D}_1^2)^{-1/4}\mathbf{D}_1(\mathbf{V}_2-\mathbf{V}_1)\end{aligned}\tag{20}$$

where

$$\begin{gathered}\mathbf{v}_1=\frac{\mathbf{V}_1}{u_0};\mathbf{V}_2=\frac{\mathbf{v}_2}{u_0};\mathbf{x}^*=\frac{\mathbf{x}}{H};\tau=\frac{tu_0}{H}\\\rho_f^*=\frac{\rho_f}{\rho_0};\rho_s^*=\frac{\rho_s}{\rho_0};\mathbf{b}_1^*=\frac{\mathbf{b}_1}{g};\mathbf{b}_2^*=\frac{\mathbf{b}_2}{g}\\\text{P}=\frac{\text{p}}{\rho_0u_0^2};\ \text{div}^*(.)=\text{H div}(.);\ \text{grad}^*(.)=\text{H grad}(.)\\\mathbf{D}^*{}_1=\frac{1}{2}\left[\text{grad}^*\mathbf{V}_1+(\text{grad}^*\mathbf{V}_1)^T\right]\\\mathbf{D}^*{}_2=\frac{1}{2}\left[\text{grad}^*\mathbf{V}_2+(\text{grad}^*\mathbf{V}_2)^T\right]\end{gathered}\tag{21}$$

where H is some characteristic length, for example half the space between the two flat plates or a tube radius, u_0 is a characteristic velocity, ρ_0 is a characteristic density, and **x** is the position vector (The asterisks have been dropped for simplicity). Finally,

$$\begin{aligned}\prod&=\frac{1+\ln(1+\kappa\dot{\gamma})}{1+\kappa\dot{\gamma}}\\\dot{\gamma}&=\left[2\,\text{tr}\,(\mathbf{D}_2^2)\right]^{1/2}\end{aligned}\tag{22a,b}$$

The following dimensionless numbers are identified:

$$\begin{gathered}\text{Re}=\frac{\rho_0u_0H}{u_f};\Lambda=\frac{\lambda_f}{\rho_0u_0H};\text{Fr}=\frac{u_0^2}{Hg}\\B_{31}=\frac{\mu_\infty}{\rho_0u_0H};B_{32}=\frac{\mu_0-\mu_\infty}{\rho_0u_0H};\\C_1=\frac{A_1}{\rho_0u_0^2};C_2=\frac{A_2H}{\rho_0u_0};C_3=\frac{A_3H^{1/2}}{\rho_0u_0^{1/2}};\end{gathered}\tag{23}$$

Where Re is the Reynolds number for the plasma, Λ is related to the second coefficient of viscosity of plasma, Fr is the Froude number, N is a prescribed number which is an average measure of the amount of particles in the system, C_1 is related to the coefficient for the forces due to density gradients, C_2 is the drag coefficient, C_3 is the lift coefficient G_1 is the gravity coefficient (a measure of the importance of gravity), B_{31}, and B_{32} are related to the viscous effects of the RBCs (similar to the Reynolds number) and **κ** is a parameter related to shear-thinning effects of the RBCs, and Π accounts for the shear-thinning effect. Our

intention is to perform a parametric study where different values of the dimensionless numbers are used.

Let us now consider the pressure driven flow of a mixture modeled by Eqn (10), (12)–(17) between two horizontal long flat plates, where X is the direction of the flow, and the plates are located at Y=-1 and Y=1 (see Figure 2). If the flow is steady and laminar, the velocity profiles and the volume fraction can be assumed to have the form:

$$\begin{aligned} \mathbf{V}_1 &= \mathrm{V}(\mathrm{Y})\mathbf{e}_x \\ \mathbf{V}_2 &= \mathrm{U}(\mathrm{Y})\mathbf{e}_x \\ \phi &= \phi(\mathrm{Y}) \end{aligned} \tag{24}$$

The equations for balance of mass are automatically satisfied. Gravity is assumed to be the only body force present. The non-dimensional momentum equations are greatly simplified by these assumptions and they can be written in component form as

$$(1-\phi)\mathrm{V}'' - \phi'\mathrm{V}' - \left(\frac{\mathrm{dP}}{\mathrm{dX}}\right)\mathrm{Re}(1-\phi) + \mathrm{C}_2\mathrm{ReF}(\phi)(\mathrm{U}-\mathrm{V}) = 0 \tag{25}$$

$$\begin{aligned} \left(\phi+\phi^2\right)\left[\mathrm{B}_{31}+\mathrm{B}_{32}\prod+\left(\mathrm{B}_{32}\frac{1}{\Gamma}\frac{\mathrm{d}\prod}{\mathrm{d}\Gamma}\mathrm{U}'^2\right)\right]\mathrm{U}'' + (1+2\phi)\phi'(\mathrm{B}_{31}+\mathrm{B}_{32}\prod)\mathrm{U}' \\ -\mathrm{C}_2\mathrm{F}(\phi)(\mathrm{U}-\mathrm{V}) - \phi\left(\frac{\mathrm{dP}}{\mathrm{dX}}\right) = 0 \end{aligned} \tag{26}$$

$$(\mathrm{P}+\mathrm{C}_1)\phi' + \left[\left(\frac{\mathrm{dP}}{\mathrm{dY}}\right) + \mathrm{G}_2 + \mathrm{C}_3\left|\mathrm{V}'\right|^{-1/2}(\mathrm{U}-\mathrm{V})\mathrm{V}'\right]\phi = 0 \tag{27}$$

$$\frac{\mathrm{dP}}{\mathrm{dY}} = -\mathrm{G}_1(1-\phi) - \mathrm{G}_2\phi \tag{28}$$

where

$$\begin{aligned} &\mathrm{F}(\phi) = 1+6.55\phi, \\ &\prod = \frac{1+\ln(1+\bar{\kappa}\Gamma)}{1+\bar{\kappa}\Gamma}, \\ &\bar{\kappa} = \frac{\kappa \mathrm{u}_0}{\mathrm{H}}, \Gamma = \frac{\mathrm{H}\dot{\gamma}}{\mathrm{u}_0}, \mathrm{G}_1 = \frac{\rho_{\mathrm{p}}}{\mathrm{Fr}}, \text{ and } \mathrm{G}_2 = \frac{\rho_{\mathrm{RBC}}}{\mathrm{Fr}}. \end{aligned} \tag{29}$$

where Γ is the dimensionless shear rate. G_1 and G_2 are dimensionless gravity coefficients. For blood with 50% hematocrit, the plasma density is 1025 g/ml and the RBC density is 1125 g/ml where the density ratio of plasma to RBC is 0.9111. Thus, G_1/G_2 is 0.9111 and only G_1 is considered as a free parameter. Overall, we have four nonlinear coupled ordinary differential equations (ODEs), which need to be solved numerically.

Based on Sugii et al. (Sugii, Okuda et al. 2005) who used micro PIV technique to measure velocity distributions of plasma and red blood cells, we select a matrix of values for the remaining parameters, summarized in Table 1.

where Q is the dimensionless volumetric flow rate of the mixture, defined as

$$Q = \int_{-1}^{1} \mathrm{V}_{\mathrm{m}}\,\mathrm{dY} = \int_{-1}^{1} \left[(1-\phi)\mathrm{V} + \phi\mathrm{U}\right]\mathrm{dY} \tag{30a}$$

It can be seen that for the reduced forms of the equations, we need three boundary conditions for V, two conditions for U, and two conditions for the volume fraction φ. We use the adherence boundary conditions on both constituents at each plate:

$$U(-1)=U(1)=V(-1)=V(1)=0 \tag{30b}$$

When the mixture is neutrally buoyant i.e., $\rho_p = \rho_{RBC} = \rho$, then $Q_m = \rho Q$. The appropriate boundary conditions for φ are the value at a plate and a prescribed average volume fraction defined through

$$N=\int_{-1}^{1} \phi \, dY \tag{31}$$

These conditions may be specified in two ways. Symmetric solutions may be obtained by specifying that $\varphi(1)$ or $\varphi(-1)$ and giving a value for N. Solutions that are in general not symmetric may be obtained if N and a value for φ on one boundary are given. This condition is expressed as

$$\phi \rightarrow \Theta \text{ as } Y \rightarrow -1 \tag{32}$$

where Θ is a constant. Then $\varphi(1)$ is determined from the solution of the equation. When gravity is included in the equations, the symmetric boundary condition, $\varphi(1)=\varphi(-1)$ is not physically possible since φ' cannot equal zero anywhere in the domain. In fact, $\varphi(-1)$ and N are specified such that$\varphi(-1) > \varphi(1)$. Numerical values for φ on the boundary could be obtained from experiments such as those performed by Segre and Silberberg (Segre and Silberberg 1962; Segre and Silberberg 1962).

Equation 25 to Equation 28 are highly nonlinear ordinary differential equations, which are solved using a collocation code (Ascher, Christiansen et al. 1981), which was found to be suitable to be more robust and more efficient than the other methods such as multiple shooting and finite difference codes (Johnson, Massoudi et al. 1991). The program implements finite element collocation methods based on piecewise polynomials for the spatial discrimination techniques. In the next section we discuss our approach to the parametric study for the various dimensionless numbers.

5. Numerical results and discussion

5.1. Effect of Reynolds number (Re)

The effects of the (plasma) Reynolds number (Re) on the velocity profiles of both constituents are shown in Figure 3. The corresponding concentration profiles are plotted in Figure 4. It can be seen that increasing Re causes a reduction of centerline velocity for plasma and RBCs, exhibited by blunting of the profiles. A similar pattern is also reported in Johnson et al. 1991(Johnson, Massoudi et al. 1991) for a mixture of granular particles and a fluid, however only the fluid velocity was blunter and the granular velocity remained parabolic. The inclusion of shear-thinning viscosity of the RBC component of the present model (Eqn 16) apparently causes this velocity to also be blunted. The degree of blunting is however disproportionate thereby resulting in a greater slip velocity indicated in Table 2 which shows the flow rates for each component. It is observed that increasing the Reynolds number results in an increase in the flow rate of plasma, but a decrease in that of RBC.

Figure 4 shows the volume fraction of RBCs (φ), for different values of Re where average volume fraction (N) is set to 0.4, which is calculated by using Eqn 31. Increasing Re causes

a non-uniform distribution of the volume fraction, as observed experimentally by Lih (Lih 1969).

5.2. Effect of average volume fraction (N)

The parameter N (related to Hct, hematocrit) is found to affect the plasma and the RBC velocity profiles differently, depending on the inclusion of shear thinning. In the absence of the shear- thinning effects ($\kappa=0$), the plasma velocity profile is blunter while the RBC velocity profile is more parabolic. (See Figure 5.) By contrast, when shear-thinning is included, increasing N results in a decrease in maximum velocity and further blunting of plasma and the RBC velocity. (See Figure 6.)

Figure 7 demonstrates that the effect of increasing the overall volume fraction of RBCs (hematocrit N) upon the concentration profile is much more pronounced above 0.1. Below this value, the concentration profile is exponential, which implies that blood can be regarded as a dilute suspension where RBC particle-particle interactions and particle-plasma interactions could be ignored (Middleman 1972). Thus, the plasma component affects the RBC velocity but not vice versa; this type of flow is called a *one-way coupling*. This assumption has been widely used in numerical simulations to understand the physical behavior of dilute particles in the field of biomedical engineering research (Kleinstreuer 2006).

5.3. Effects of κ, B_{31}, and B_{32}

Figure 8 shows the velocity profiles for values of κ ranging from 0.1 to 1000. The centerline velocity of RBCs is found to increase with increasing κ, gradually becoming parabolic as κ approaches 1000. A similar pattern for the mean velocity of the mixture shown in Figure 9, is also found in Yeleswarapu (Yeleswarapu 1994). The non-dimensional mean velocity can be calculated using the following equation

$$V_m=(1-\phi)V+\phi U \tag{33}$$

where V_m is the non-dimensional mixture velocity, V is the non-dimensional plasma velocity, U is the non-dimensional RBC velocity, and φ is the volume fraction of the RBC component. As κ approaches infinity, the viscosity depends on B_{31}, which implies that the fluid behaves as a Newtonian fluid. Thus, it is observed in Figure 8 and Figure 9 that both plasma and RBC velocities become more parabolic. Conversely, increasing κ represents greater shear-thinning, leading to increased bluntness of the velocity profile.

Figure 9 illustrates the influence of κ upon the concentration profile of RBCs (the F–L effect.) As κ approaches 0.1, there is approximately a 12% depletion of RBCs near the wall and a 7% excess at the centerline. When κ is much greater than 100, the variation from core to wall decreases below 2%, and becomes nearly uniform.

Figure 10 shows the effect of B_{31}. In this range, i.e., from 10 to 100, there is negligible influence on the velocity and the volume fraction distribution. By contrast, a 6 times change in B_{32} causes a far more prominent effect on the bluntness of the velocity distribution and the near-wall depletion of RBCs (See Figure 11). A similar pattern is found in Yeleswarapu (Yeleswarapu 1994).

5.4. Effect of the gravitational parameter (G_1)

Additional simulations were performed in which the gravitational parameter G_1 was varied from 0.1 to 10. Figure 12 shows the velocity profiles and the volume fraction for two values of the dimensionless gravity coefficient G_1 without lift force where the dimensionless lift

coefficient (C_3) is set to zero. Increasing G_1 is observed to cause a non-symmetric velocity profile for both the plasma and the RBCs; thus $\varphi(-1) \neq \varphi(1)$. This observation is also reported in Johnson et al. (Johnson, Massoudi et al. 1991) who found that the particle velocity became skewed towards the lower plate. The volume fraction distribution is affected in a similar fashion. At the upper plate (Y=1) it is seen that φ decreases as G_1 increases, indicating a translocation of RBCs in the direction of the gravity force. This effect is unlikely to be observable at Reynolds > 1, as the magnitude of the gravitational force is one tenth or less of the drag force

It is interesting to note that the addition of the (shear) lift force creates the opposite effect to that of gravity. (See Figure 13.) Under these conditions, the RBC velocity is skewed away from the lower plate towards the upper plate. However, the RBC volume fraction was skewed towards the bottom wall (in the direction of gravity) as observed in the previous case (without the lift force). (See Figure 12.) Experimental observation (Fahraeus 1929) shows that RBCs migrate towards the center and collect there (symmetrically). This indicates that the magnitude of gravity is much smaller than that of lift force to cause the migration of the RBCs.

When the lift force is more dominant than the gravity, that is for larger values of C_2, the velocity profile becomes more parabolic. It is also observed in Figure 14 that the lift force has a significant role in causing a decrease between the plasma velocity and the RBCs velocity. The RBCs distribution could vary from a uniform distribution to a symmetrical one due to the dominant effect of the lift force when compared to gravity. However, as G_1 increases, the RBCs are distributed more non-uniformly (Figure 15). This observation is also found in Johnson et al (Johnson, Massoudi et al. 1991).

5.5. Effect of the diffusion coefficient (C_1)

Figure 16 indicates that as the value of the density gradient coefficient C_1 becomes larger, both plasma and RBC velocity profiles become more parabolic and the centerline slip velocity between the two constituents increases. In addition, as C_1 increases the RBCs volume fraction becomes more uniform, effectively counteracting the influence of lift and drag (See Figure 17). Based on the numerical observations it can be implied that the magnitude of the diffusion force could be less than that of the lift force.

5.6. Effect of the drag coefficient (C_2)

Similar to the effect of diffusion, the influence of the drag coefficient is to cause the velocity profiles of the plasma and the RBCs to be more parabolic, and the RBCs distribution to be more uniform. (See Figure 18 and Figure 19.) Unlike the case for increasing the diffusion term, increasing the drag coefficient (C_2) results in an increase in the slip velocity.

5.7. Effect of the lift coefficient (C_3)

A parametric study of the lift coefficient C_3 in the range of 1 to 100 was performed and it is observed to minimally influence the velocity profiles of RBCs and plasma, but dramatically affects the RBCs distribution. Increasing C_3 by a factor of 10 (from 1 to 10 and 10 to 100) greatly accentuated the near-wall depletion of RBCs, causing them to collect toward the core (See Figure 20 and Figure 21). Experimental and numerical observations demonstrate that RBCs migrate towards the tube axis (Bloch 1962; Goldsmith (1971); Zhao, Marhefka et al. 2008; Zhang, Johnson et al. 2009). In Figure 20, it can be seen that as C3 increases, there is an, albeit small, reduction in the plasma velocity in regions of higher RBCs concentration and an increase in the plasma velocity in the regions of lower RBCs concentration. That is, the RBCs move slower in the regions of higher concentration and faster in the regions of lower concentration.

Nonlinear distribution of the volume fraction causes an increase in the plasma velocity near the walls where the RBCs volume fraction decreases and a decrease in the plasma velocity where the RBCs concentration increases (Figure 22 and Figure 23).

6. Concluding remarks

The constitutive equation used in our study for the stress tensor of the RBCs is assumed to be isotropic, but in reality the RBCs are anisotropic and deformable. The difficulty is the orientation or the alignment of the non-spherical cells (Chien, Usami et al. 1967; Zhao, Marhefka et al. 2008). This could be addressed an anisotropic representation for the RBCs, as proposed by Massoudi and Antaki (Massoudi and Antaki 2008), in which the stress tensor is a function of the symmetric part of velocity gradient, $\mathbf{D}_2$, and the orientation vector, $\mathbf{n}$. This was not employed here as it would have introduced yet additional governing conservation equations such as the balance of angular momentum, additional boundary conditions, and associated constitutive parameters (Massoudi 2005; Massoudi and Antaki 2008). It is nevertheless a worthy topic of future study.

According to Muller (Muller 1968), a force of the type $C_1 \text{grad}\, \varphi$, must be included in the interaction forces for the problem of multi-component flows to be well-posed. We also observe the important role of the diffusion term in the numerical simulations. Especially when the lift force is included, the diffusion term is critically important to make the simulations stable. A similar numerical observation is also found in Johnson et al (1991a,b) in which the gradient of the volume fraction of the granular component, similar to the diffusion was found necessary for stability of the simulations. We also notice another important relationship between C_1, C_2, and C_3 from the sensitivity studies performed here. If C_3/C_2 is greater than C_1, the numerical simulations are unstable. In general, it is found that C_1 should be an order of magnitude greater than C_3/C_2 to assure numerical stability. This can be used to provide a limiting value of the diffusion coefficient for future 3-dimensional simulations.

There have been no investigations pointing to the form of A_1 (or C_1) in Eqn 17. The remaining coefficients have been studied to a limited extent for the general two-component flows. Thus, the forms given above are ad-hoc and they are perhaps valid under strict conditions. The forms given to the coefficient of the interaction forces are either generalization of a single particle result or due to some other limiting conditions.

Furthermore, many of the dimensionless numbers defined in Eqn 22 would not be correct or appropriate for non-spherical particles such as fibers or blood cells. Despite the assumptions involved, these expressions in many ways effectively describe how the interaction forces vary with the system parameters. Another limitations of the constitutive equations for the RBC component is the lack of explicit consideration of RBCs aggregation (Chien, Usami et al. 1967) and elasticity (Thurston 1972; Thurston 1993). Instead, these phenomena have been incorporated into a shear thinning viscosity function, which in turn is based on experiments in whole blood.

When blood flows through a micro-scale tube, it is observed that under certain conditions the red blood cells (RBCs) migrate away from the wall of the tube and concentrate toward the center of the tube, thus causing a cell-free layer near the wall, called the plasma-skimming layer. The other observed phenomenon is the reduction of the apparent viscosity near the wall. Both experimental observations were reported first by Fahraeus and Lindqvist (Fahraeus 1929; Fahraeus and Lindqvist 1931). One of the limitations in our study is that the RBC cell free layer is not exhibited. No theoretical studies have been able to describe this phenomenon. One possibility solution could be to consider a modified viscosity model

proposed by Yeleswarapu, which could be a function of RBC concentration as well as the shear rate. As seen experimentally, the RBC viscosity should approach zero near the wall due to the depletion of the RBCs. The other possibility is to consider a modified lift force or to add another force due to the wall effect also called a *lubricant effect*. This might cause infinite force acting on the RBCs when they approach the wall, thus resulting in the RBC depletion near wall. From the current study, we conclude that the drag and lift forces are the most important ones for hemodynamics applications. Thus, the next step is to focus on improving or identifying better forms for the interaction forces (Crowe, Sommerfeld et al. 1997; Clift, Grace et al. 2005; Fan 2005). For the future studies, we intend to consider the complete model shown in Eqn 11.

Highlights

- A modified form of the mixture theory is used to study the blood flow in a simple geometry, namely flow between two plates.
- The blood is assumed to behave as a two-component mixture comprised of plasma and red blood cells (RBCs).
- Plasma is tacit to behave as gluey fluid but RBCs given granular-like structure where viscosity also depends on shear-rate.

Acknowledgments

This project was supported by NIH R01 HL089456-01.

Glossary

Nomenclature:

a	acceleration vector
b	body force vector
D	symmetric part of the velocity gradient
I	identity tensor
L	gradient of velocity vector
p	fluid pressure
T	stress tensor
v	velocity vector
W	spin tensor
x	position vector

Greek Letters

λ_f	second coefficient of viscosity
μ	first coefficient of viscosity
ρ	density
ρ_o	reference density

φ volume fraction

Subscripts

1 referring to the constituent 1 (→plasma)

2 referring to the constituent 2 (→Red Blood Cells)

m referring to the mixture

Superscripts

T transpose

Other Symbols

div divergence operator

∇ gradient operator

tr trace of a tensor

$\otimes$ outer product

. dot (scalar) product

References

ANSYS FLUENT 12.0 User Guide.

Aarts P, Vandenbroek SAT, et al. Blood-platelets are concentrated near the wall and red blood-cells, in the center in flowing blood. Arteriosclerosis. 1988; 8(6):819–824. [PubMed: 3196226]

Adkins JE. Non-Linear Diffusion, 1. Diffusion and Flow of Mixtures of Fluids. Phil. Trans. Roy. Soc. London A. 1963; 255:607–633.

Adkins JE. Non-Linear Diffusion, 2. Constitutive Equations for Mixtures of Isotropic Fluids. Phil. Trans. Roy. Soc. London A. 1963; 255:635–648.

Anderson TB, Jackson R. A fluid mechanical description of fluidized beds. Industrial & Engineering Chemistry Fundamentals. 1967; 6(4) 527-&.

Araujo RP, Mcelwain DLS. A mixture theory for the genesis of residual stresses in growing tissues I. Siam Journal on Applied Mathematics. 2005; 65 1261-

Araujo RP, McElwain DLS. A mixture theory for the genesis of residual stresses in growing tissues II: solutions to the biphasic equations for a multicell spheroid. Siam Journal on Applied Mathematics. 2006; 66(2):447–467.

Ascher U, Christiansen J, et al. Collocation software for boundary-value ODEs. Acm Transactions on Mathematical Software. 1981; 7(2):209–222.

Ateshian GA. On the theory of reactive mixtures for modeling biological growth. Biomechanics and Modeling in Mechanobiology. 2007; 6(6):423–445. [PubMed: 17206407]

Ateshian GA, Likhitpanichicul M, et al. A mixture theory analysis for passive transport in osmotic loading of cells. Journal of Biomechanics. 2006; 39(3):464–475. [PubMed: 16389086]

Atkin RJ, Craine RE. Continuum theories of mixtures: Applications. J. Inst. Math. Applications. 1976; 17:153–207.

Atkin RJ, Craine RE. Continuum theories of mixtures: Basic theory and historical development. Quart. Jour. Mech. and Appl. Math. 1976; 29:209–244.

Axtell NK, Park M, et al. Micromorphic fluid in an elastic porous body: Blood flow in tissues with microcirculation. International Journal for Multiscale Computational Engineering. 2005; 3(1):71–83.

Bagchi P. Mesoscale simulation of blood flow in small vessels. Biophysical Journal. 2007; 92(6): 1858–1877. [PubMed: 17208982]

Bedford A, Drumheller DS. Recent advances: theories of immiscible and structured mixtures. Int. J. Engng. Sci. 1983; 21:863–960.

Bloch EH. A quantitative study of hemodynamics in living microvascular system. American Journal of Anatomy. 1962; 110(2) 125-&.

Bowen, RM., editor. Theory of mixtures. Continuum Physics. New York: Academic; 1976.

Bugliarello G, Kapur C, et al. The profile viscosity and other characteristics of blood flow in a non-uniform shear field. (Proc. 4th Int. Rheol. Conf).

Carr RT, Wickham LL. Plasma skimming in serial microvascular bifurcations. Microvascular Research. 1990; 40(2):179–190. [PubMed: 2250597]

Chien S, Usami S, et al. Effects of hematocrit and plasma proteins on human blood rheology at low shear rates. Journal of Applied Physiology. 1966; 21(1) 81-&.

Clift, R.; Grace, JR., et al. Bubbles, drops, and particles. Dover Publications; 2005.

Collins IF. Elastic/plastic models for soils and sands. Int. J. Mech. Sci. 2005; 47:493–508.

Crowe, C.; Sommerfeld, M., et al. Multiphase flows with droplets and particles. CRC Press; 1997.

Drew DA, Segel LA. Averaged equations for 2-phase flows. Studies in Applied Mathematics. 1971; 50(3) 205-&.

Fahraeus R. The suspension stability of the blood. Physiological Reviews. 1929; 9(2):241–274.

Fahraeus R, Lindqvist T. The viscosity of the blood in narrow capillary tubes. American Journal of Physiology. 1931; 96(3):562–568.

Fan, LS. Principles of Gas-Solid Flows. Cambridge University Press; 2005.

Fung, YC. Biomechanics: Mechanical Properties of Living Tissues. Springer; 1993.

Galdi, GP.; Rannacher, R., et al. Hemodynamical Flows: Modeling, Analysis and Simulation. Birkhäuser Basel; 2008.

Garikipati K, Arruda EM, et al. A continuum treatment of growth in biological tissues: The coupling of mass transport and mechanics. J. Mech. Phys. Solids. 2004; 52:1595–1625.

Gidaspow, D. Multiphase Flow and Fluidization: Continuum and Kinetic Theory Descriptions. Academic Press; 1994.

Goldsmith HL. Red cell motions and wall interactions in tube flow. Federation Proceedings. 1971; 30(5) 1578-&.

Goldsmith HL, Takamura K, et al. Shear-induced collisions between human-blood cells. Annals of the New York Academy of Sciences 416(DEC). 1983:299–318.

Gu WY, Lai WM, et al. A mixture theory for charged-hydrated soft tissues containing multi-electrolytes: Passive transport and swelling behaviors. Journal of Biomechanical Engineering-Transaction of the ASME. 1998; 120(2):169–180.

Humphrey, JD.; DeLange, S. An Introduction to Biomechanics: Solids and Fluids. Analysis and Design Springer; 2004.

Humphrey JD, Rajagopal KR. A constrained mixture model for growth and remodeling of soft tissues. Mathematical Models & Methods in Applied Sciences. 2002; 12:407–430.

Hyun S, Kleinstreuer C, et al. Hemodynamics analyses of arterial expansions with implications to thrombosis and restenosis. Medical Engineering & Physics. 2000; 22(1):13–27. [PubMed: 10817945]

Ishii M. Thermo-Fluid Dynamic Theory of Two-Phase Flow Eyrolles. 1975

Johnson G, Massoudi M, et al. A Review of Interaction Mechanisms In Fluid-Solid Flows, DOE/PETC/TR-90/9. 1990

Johnson G, Massoudi M, et al. Flow of a fluid infused with solid particles through a pipe. International Journal of Engineering Science. 1991; 29(6):649–661.

Johnson G, Massoudi M, et al. Flow of a fluid solid mixture between flat plates. Chemical Engineering Science. 1991; 46(7):1713–1723.

Jung J, Hassanein A. Three-phase CFD analytical modeling of blood flow. Medical Engineering & Physics. 2008; 30(1):91–103. [PubMed: 17244522]

Jung JH, Hassanein A, et al. Hemodynamic computation using multiphase flow dynamics in a right coronary artery. Annals of Biomedical Engineering. 2006; 34(3):393–407. [PubMed: 16477502]

Kesmarky G, Kenyeres P, et al. Plasma viscosity: A forgotten variable. Clinical Hemorheology and Microcirculation. 2008; 39(1–4):243–246. [PubMed: 18503132]

Kleinstreuer, C. Biofluid Dynamics: Principles and Selected Applications. CRC Press; 2006.

Klisch SM, Lotz JC. A special theory of biphasic mixtures and experimental results for human annulus fibrosus tested in confined compression. ASME J. Biomech. Engng. 2000; 122:180–188.

Kuhn S, Hauger W. A theory of the adaptive growth of biological materials. Archive of Applied Mechanics. 2000; 70(1–3):183–192.

Lai WM, Hou JS, et al. A triphasic theory for the swelling and deformation behaviors of articular-cartilage. Journal of Biomechanical Engineering-Transaction of the ASME. 1991; 113(3):245–258.

Lemon G, King JR, et al. Mathematical modelling of engineered tissue growth using a multiphase porous flow mixture theory. J. Math. Biol. 2006; 52:571–594. [PubMed: 16463188]

Lih MM. A mathmatical model for axial migration of suspended particles in tube flow. Bulletin of Mathematical Biophysics. 1969; 31(1) 143-&.

Massoudi, M. Application of Mixture Theory to Fluidized Beds. Unviersity of Pittsburgh; 1986. Ph.D. Dissertation

Massoudi M. Stability analysis of fluidized beds. International Journal of Engineering Science. 1988; 26(7):765–769.

Massoudi M. On the flow of granular materials with variable material properties. International Journal of Non-Linear Mechanics. 2001; 36(1):25–37.

Massoudi M. On the importance of material frame-indifference and lift forces in multiphase flows. Chemical Engineering Science. 2002; 57(17):3687–3701.

Massoudi M. Constitutive relations for the interaction force in mmulticomponent particulate flows. Internatinal Journal of Non-Linear Mechanics. 2003; 38:316–336.

Massoudi M. An anisotropic constitutive relation for the stress tensor of a rodlike (fibrous-type) granular material. Mathematical Problems in Engineering. 2005; (6):679–702.

Massoudi M. Boundary conditions in mixture theory and in CFD applications of higher order models. Computers & Mathematics with Applications. 2007; 53(2):156–167.

Massoudi M. A note on the meaning of mixture viscosity using the classical continuum theories of mixtures. International Journal of Engineering Science. 2008; 46(7):677–689.

Massoudi M. A Mixture Theory formulation for hydraulic or pneumatic transport of solid particles. International Journal of Engineering Science. 2010; 48(11):1440–1461.

Massoudi M, Antaki JF. An anisotropic constitutive equation for the stress tensor of blood based on Mixture Theory. Mathematical Problems in Engineering. 2008; 2008 Article ID 579172, 31 pages.

Massoudi M, Johnson G. On the flow of a fluid-particle mixture between two rotating cylinders, using the theory of interacting continua. International Journal of Non-Linear Mechanics. 2000; 35(6): 1045–1058.

Massoudi M, Rajagopal KR, et al. Remarks on the modeling of fluidized systems. AIChE Journal. 1992; 38(3):471–472.

Massoudi M, Rajagopal KR, et al. On the fully developed flow of a dense particulate mixture in a pipe. Powder Technology. 1999; 104(3):258–268.

Massoudi M, Rao CL. Vertical flow of a multiphase mixture in a channel. Mathematical Problems in Engineering. 2001; 6(6):505–526.

Middleman, S. Trasport phenomena in the cardiovascular system. Wiley-Interscience; 1972.

Mow VC, Holmes MH, et al. Fluid transport and mechanical properties of articular cartilage: a review. J. Biomech. 1984:377–394. [PubMed: 6376512]

Mow VC, Kuei SC, et al. Biphasic creep and stress relaxation of articular cartilage in compression? Theory and experiments. J. Biomech. Eng. 1980; 102(1):73–84. [PubMed: 7382457]

Muller I. A thermodynamic theory of mixtures of fluids. Archive for Rational Mechanics and Analysis. 1968; 28(1) 1-&.

Muller I. The influecne of density graients on forces in a mixture. J. Non-Equilb. Theromodyn. 1977; 2:133–138.

Pal R. Rheology of concentrated suspensions of deformable elastic particles such as human erythrocytes. Journal of Biomechanics. 2003; 36(7):981–989. [PubMed: 12757807]

Rajagopal KR. On a hierarchy of approximate models for flows of incompressible fluids through porous solids. Math. Models Meth. Appli. Sci. 2007; 17:215–252.

Rajagopal KR, Massoudi M, et al. Flow of granualar-materials between rotating disks. Mechanics Research Communications. 1994; 21(6):629–634.

Rajagopal, KR.; Tao, L. Mechanics of Mixtures. Singapore: World Scientific Publishing; 1995.

Rajagopal KR, Troy W, et al. Existence of solutions to the equations governing the flow of granular materials. European Journal of Mechanics B-Fluids. 1992; 11(3):265–276.

Ravindran P, Anand NK, et al. Steady free surface flow of a fluid-solid mixture down an inclined plane. Particulate Science and Technology. 2004; 22(3):253–273.

Samohyl, I. Thermomechanics of Irreversible Processes in Fluid Mixtures. Tuebner, Leipzig; 1987.

Segre G, Silberberg A. Behaviour of macroscopic rigid spheres in Poiseuille flow Part 1. Determination of local concentration by statistical analysis of particle passages through crossed light beams. Journal of fluid mechanics. 1962; 14:115–135.

Segre G, Silberberg A. Behaviour of macroscopic rigid spheres in Poiseuille flow Part 2. Experimental results and interpretation. Journal of fluid mechanics. 1962; 14:136–157.

Sharan M, Popel AS. A two-phase model for flow of blood in narrow tubes with increased effective viscosity near the wall. Biorheology. 2001; 38(5–6):415–428. [PubMed: 12016324]

Sugii Y, Okuda R, et al. Velocity measurement of both red blood cells and plasma of in vitro blood flow using high-speed micro PIV technique. Measurement Science & Technology. 2005; 16(5): 1126–1130.

Tao L, Humphrey JD, et al. A mixture theory for heat-induced alterations in hydration and mechanical properties in soft tissues. Int. J. Engng. Sci. 2001; 39:1535–1556.

Thurston GB. Viscoelasticity of human blood. Biophysical Journal. 1972; 12(9) 1205-&.

Thurston GB. Frequency and shear rate dependence of viscoelasticity of human blood. Biorheology. 1973; 10(3):375–381. [PubMed: 4772010]

Thurston GB. The elastic yield stress of human blood. Biomedical Sciences Instrumentation. 1993:87–93. [PubMed: 8329640]

Truesdell C. Sulle basi della thermomeccanica. Rand Lincei, Series. 1957; 8:22. 33–38, and 158–166.

Truesdell, C. Rational Thermodynamics. Springer-Verlag; 1984.

Yeleswarapu, KK. Evaluation of continuum models for characterizing the constitutive behavior of blood. University of Pittsbugh; 1994. PhD dissertation

Yeleswarapu KK, Kameneva MV, et al. The flow of blood in tubes: theory and experiment. Mechanics Research Communications. 1998:25.

Zhang JF, Johnson PC, et al. Effects of erythrocyte deformability and aggregation on the cell free layer and apparent viscosity of microscopic blood flows. Microvascular Research. 2009; 77(3):265–272. [PubMed: 19323969]

Zhao R, Marhefka JN, et al. Micro-flow visualization of red blood cell-enhanced platelet concentration at sudden expansion. Annals of Biomedical Engineering. 2008; 36(7):1130–1141. [PubMed: 18418710]

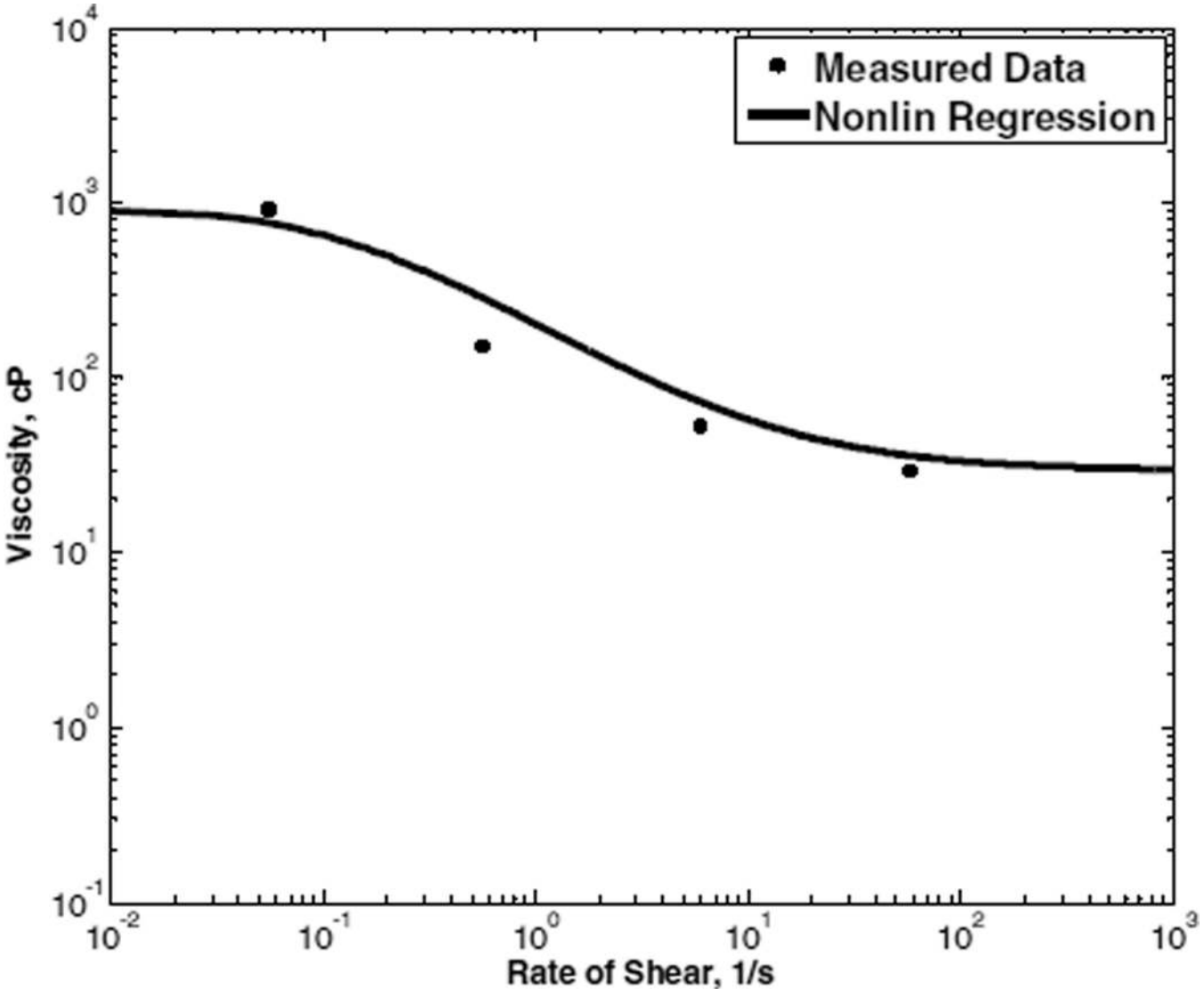

Figure 1.
Shear thinning model for viscosity of RBC phase, calibrated to experimental data of Chien et al (1966) (Chien, Usami et al. 1966) for 90% Ht.

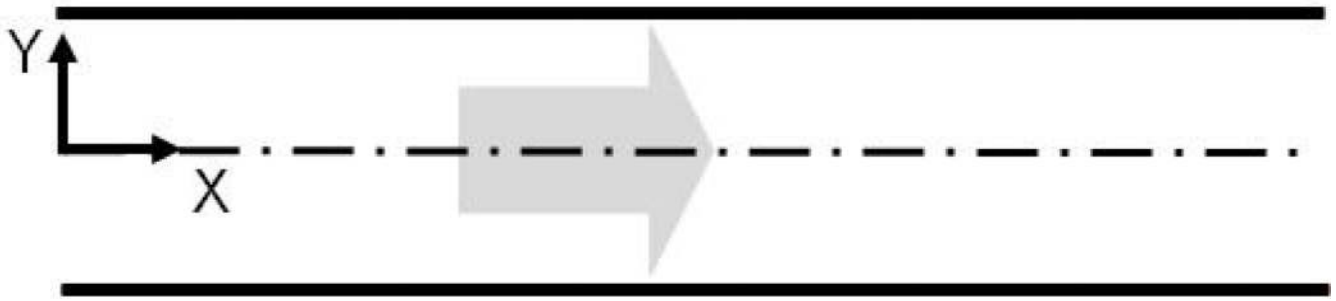

Figure 2.
Flow between parallel plates located at Y=−1 and Y=1.

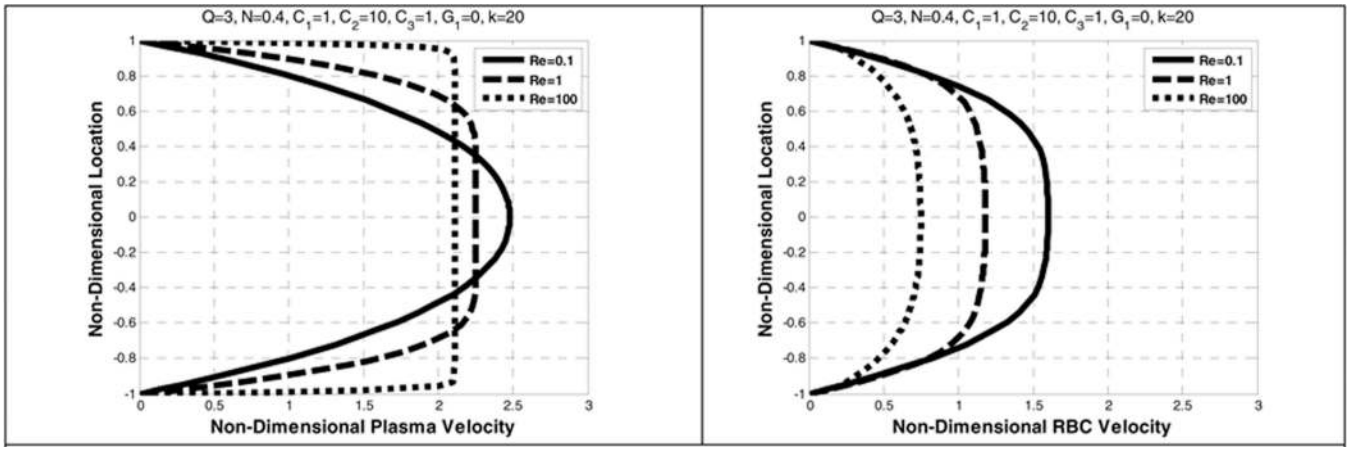

Figure 3.
Effect of Reynolds number (Re) on the plasma velocity (left) and the RBC velocity (right)

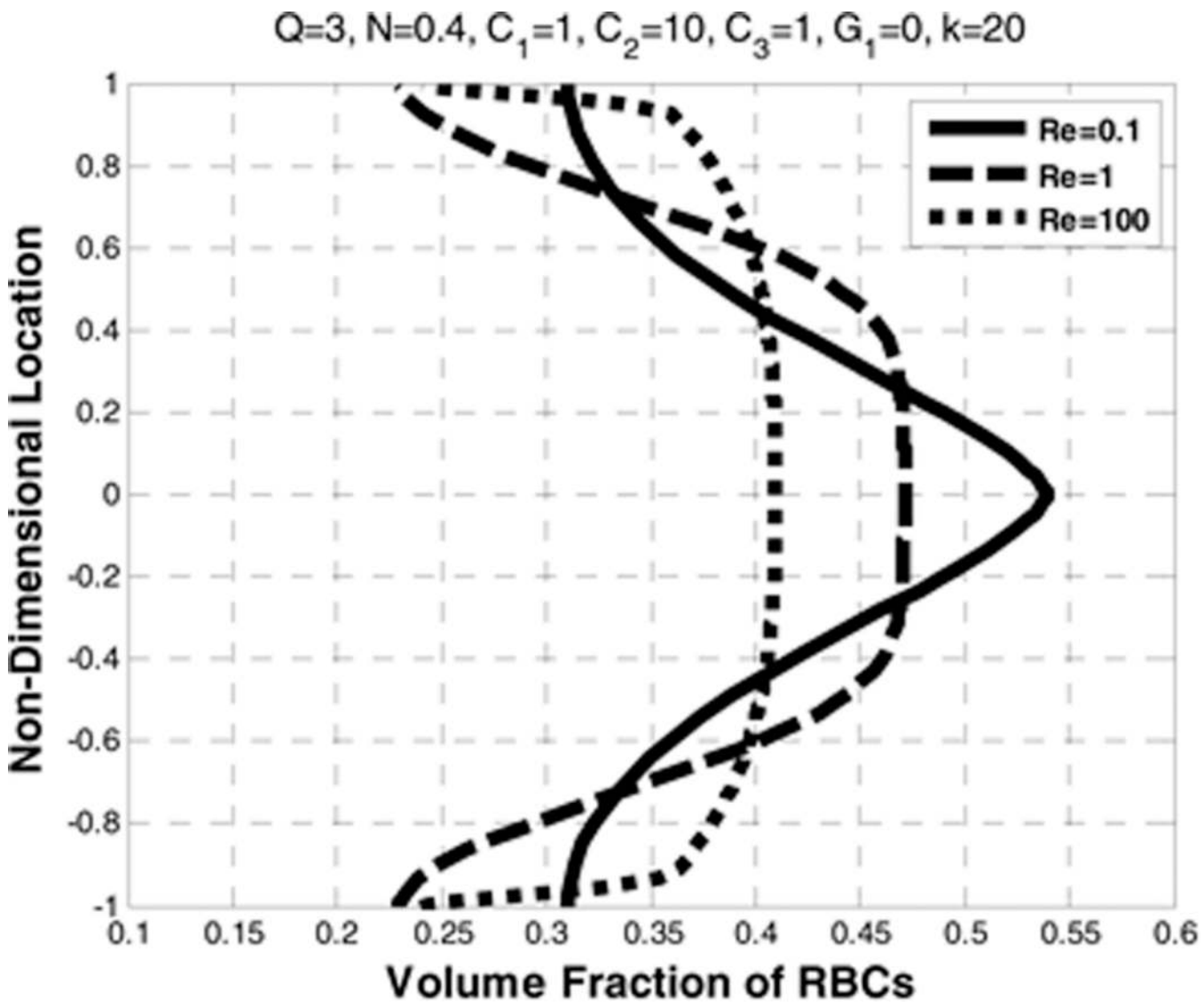

Figure 4.
Effect of Reynolds number (Re) on the volume fraction of RBCs

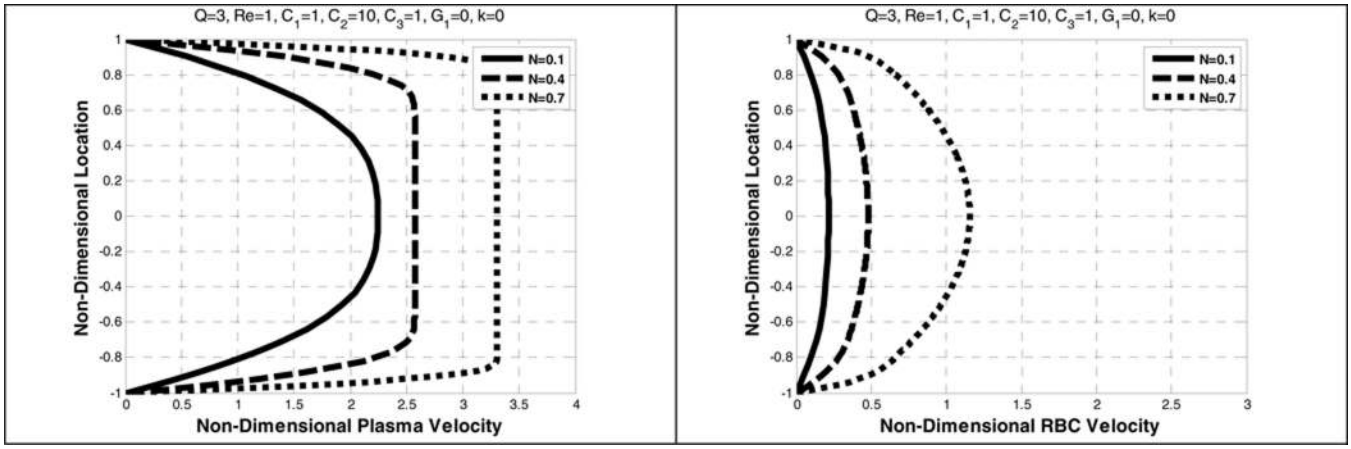

Figure 5.
Effect of average volume fraction (N) on the plasma velocity (left) and the RBC velocity (right), without shear-thinning

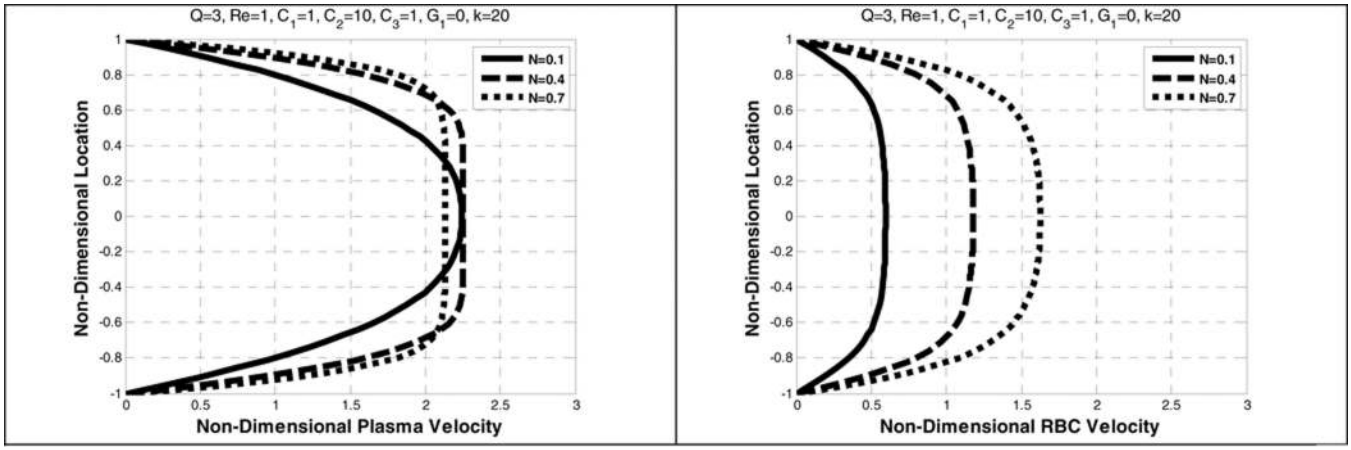

Figure 6.
Effect of average volume fraction (N) on the plasma velocity (left) and the RBC velocity (right) with shear-thinning

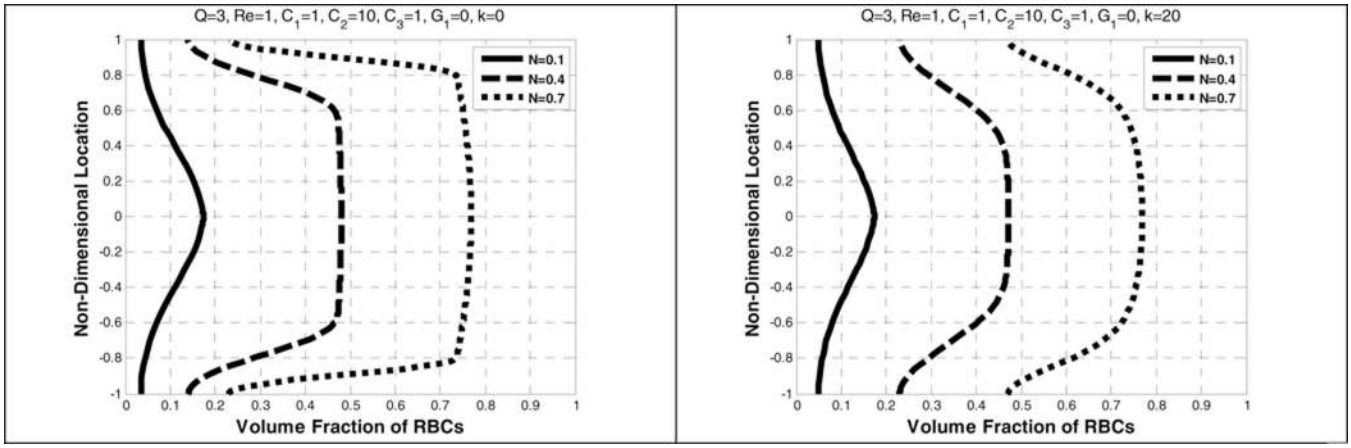

Figure 7.
Effect of average volume fraction (N) on the volume fraction of RBCs without a shear-thinning (left) and with a shear-thinning (right)

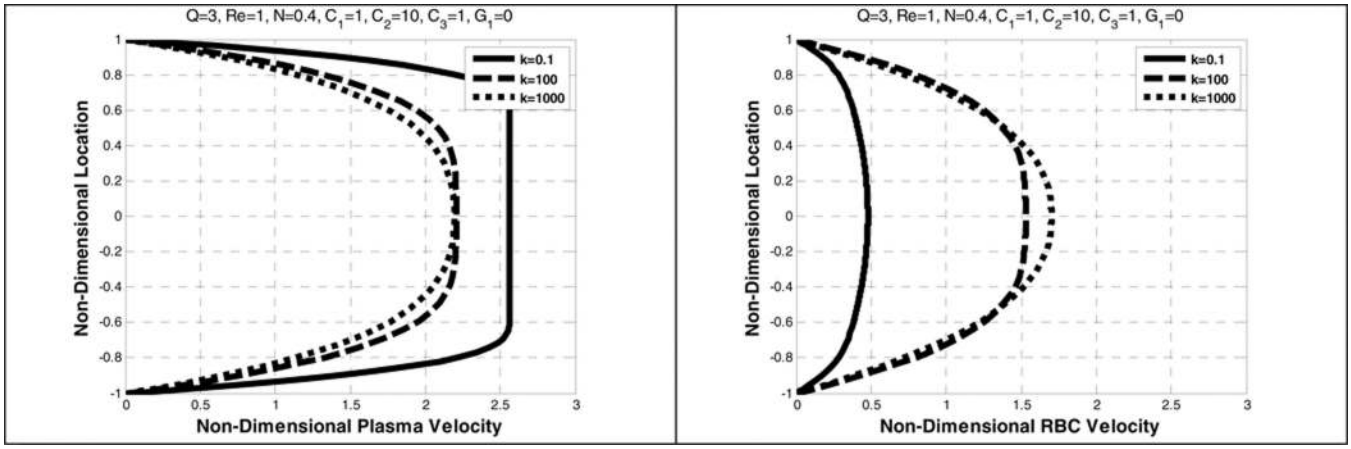

Figure 8.
Effect of the material constant (κ) on the plasma velocity (left) and the RBC velocity (right).

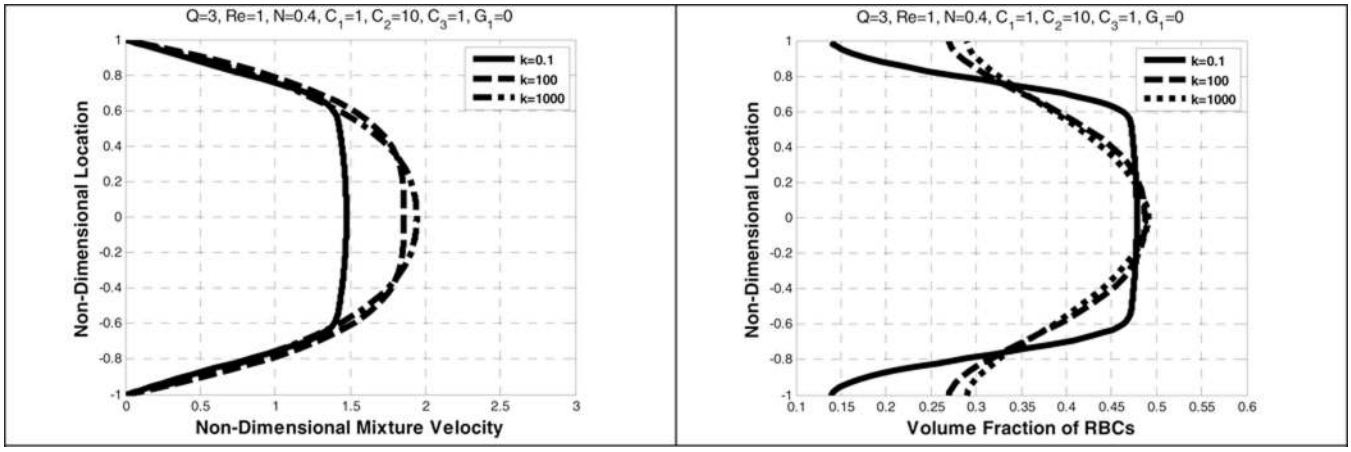

Figure 9.
Effect of the material constant (κ) on the mean velocity of the mixture and the volume fraction of RBCs

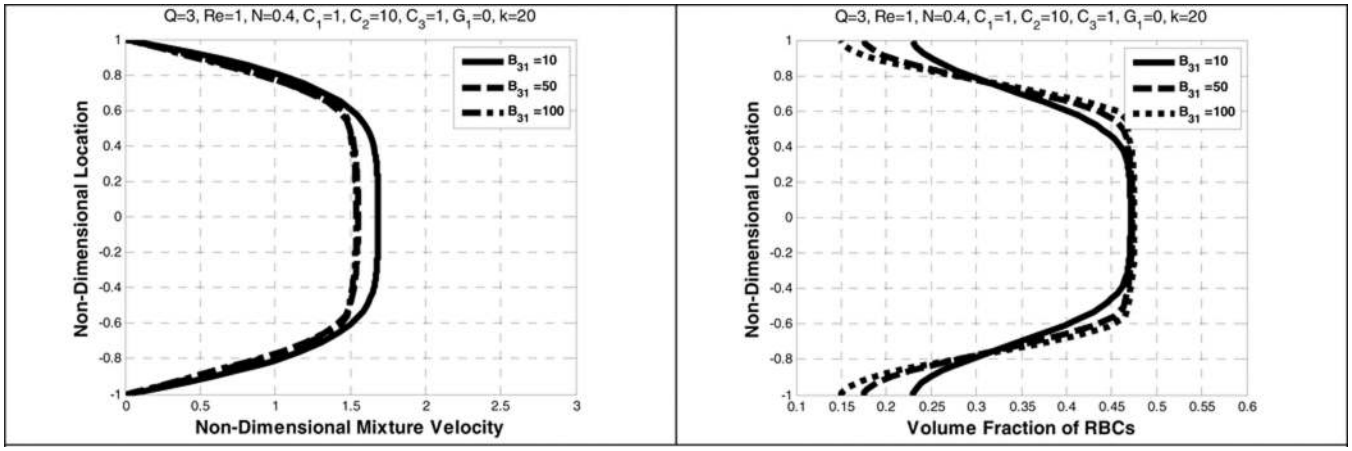

Figure 10.
Effect of B_{31} on the mixture velocity (left) and the volume fraction of RBCs (right).

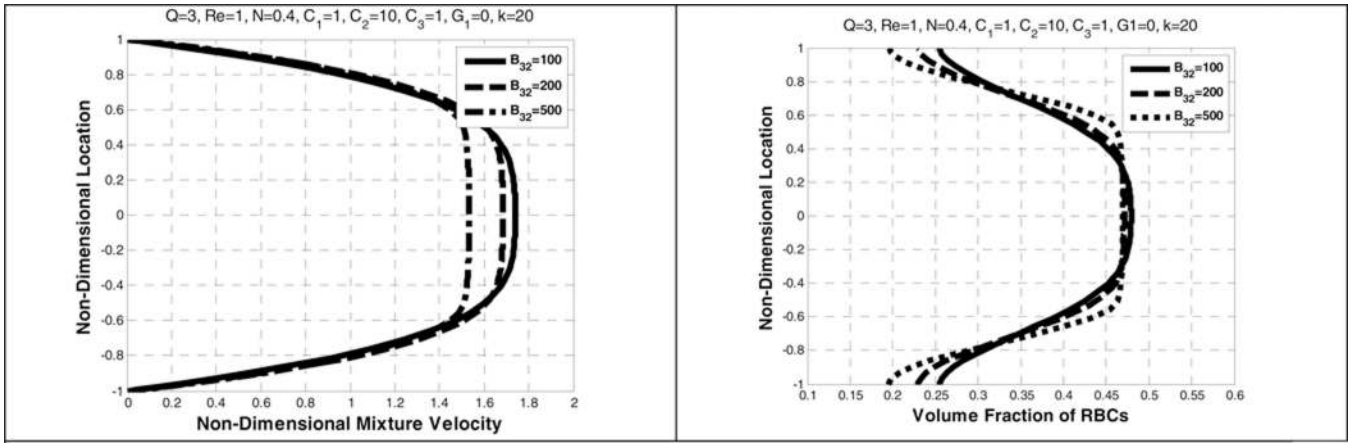

Figure 11.
Effect of B_{32} on the mixture velocity (left) and the volume fraction of RBCs (right).

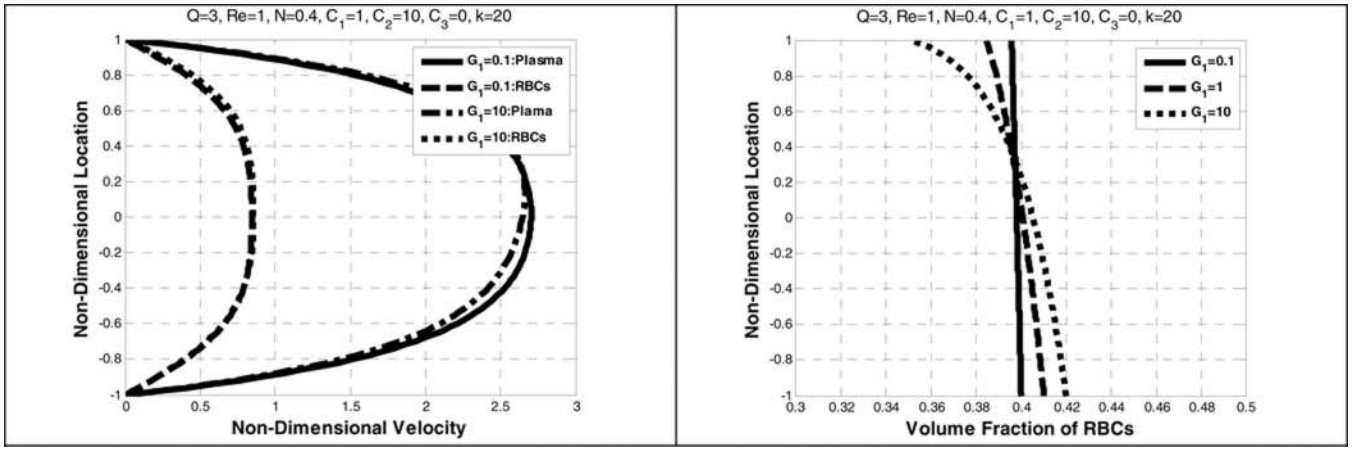

Figure 12.
Effect of dimensionless gravity (G_1) on the plasma and RBC velocity profiles (left) and the volume fraction of RBCs (right)

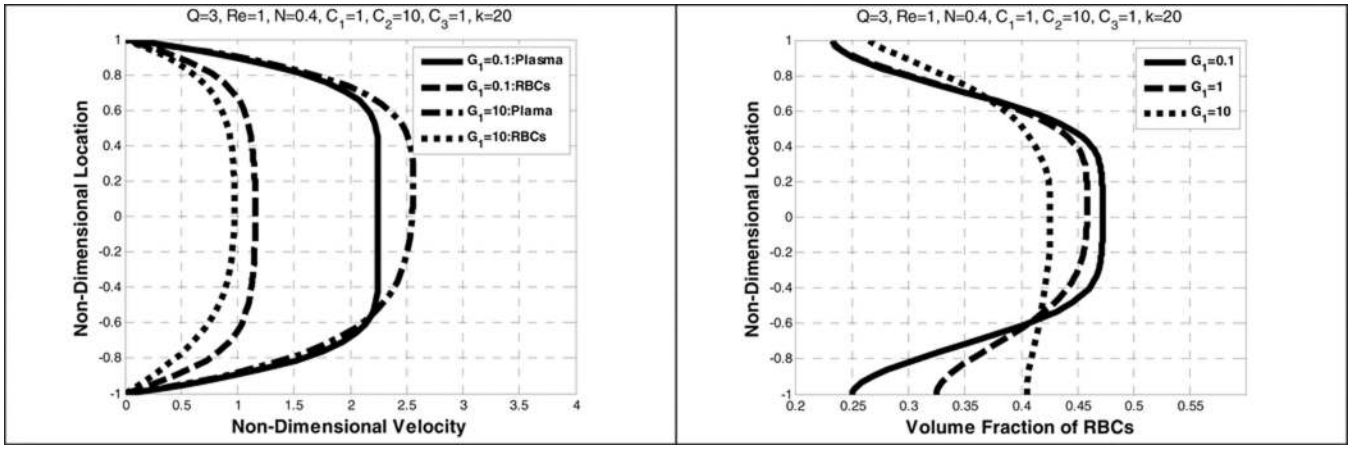

Figure 13.
Effect of combination of dimensionless gravity and shear lift on plasma and RBC velocity profile (left) and the volume fraction of RBCs (right)

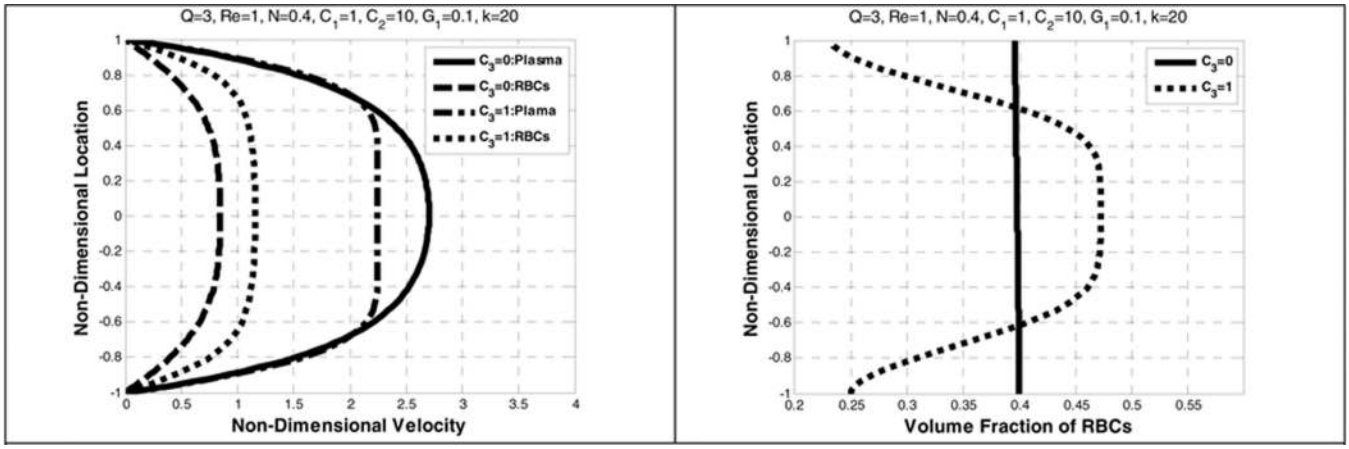

Figure 14.
Effect of lift coefficient (C_3) on the plasma and RBC velocities (left) and the volume fraction of RBCs (right)

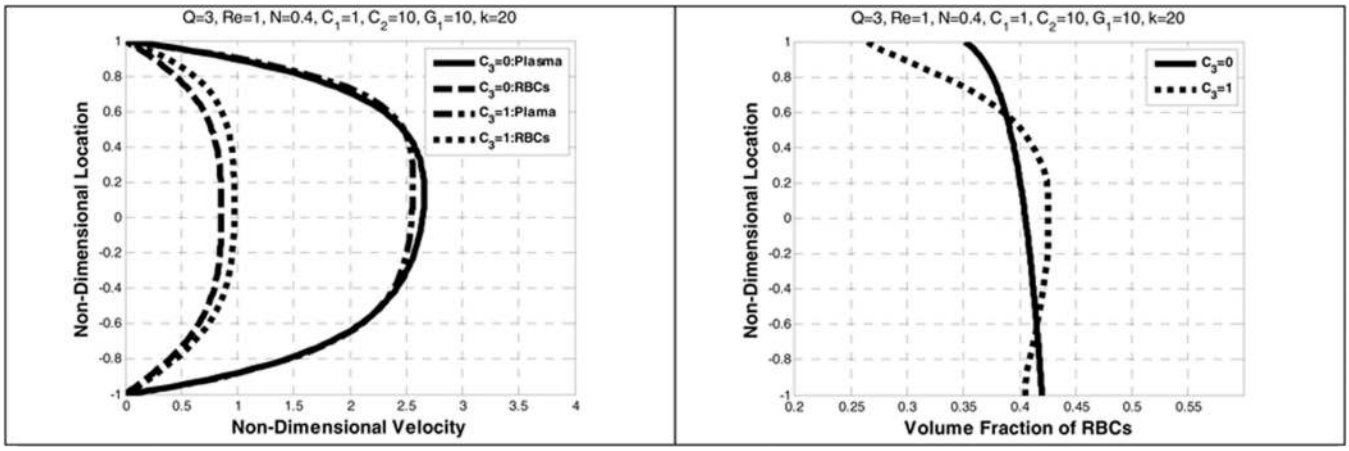

Figure 15.
Effect of lift coefficient (C_3) on the plasma and RBC velocities (left) and the volume fraction of RBCs (right)

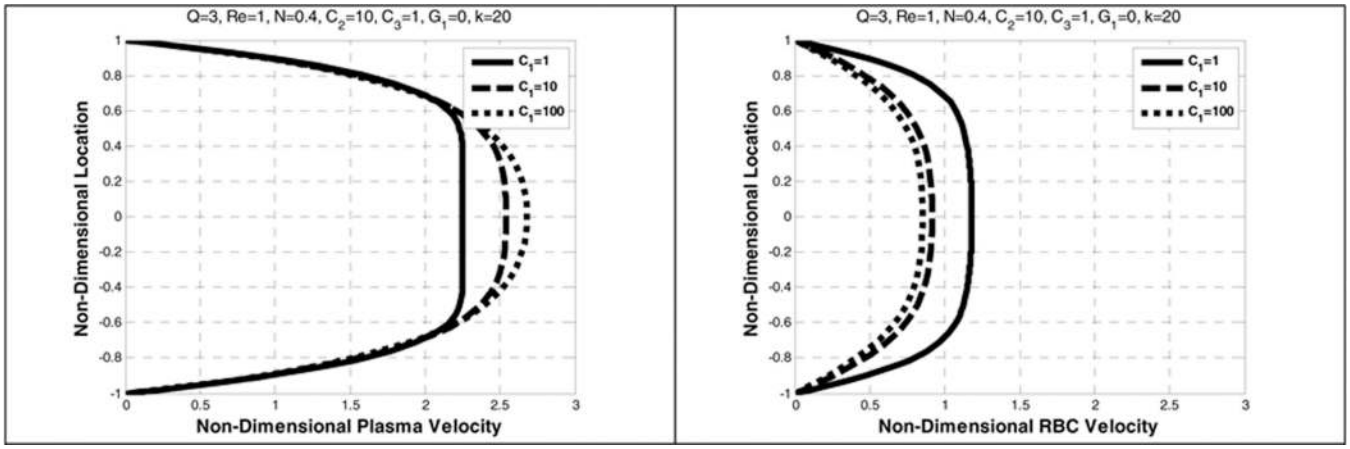

Figure 16.
Effect of density gradient coefficient (C_1) on the plasma velocity (left) and the RBC velocity (right).

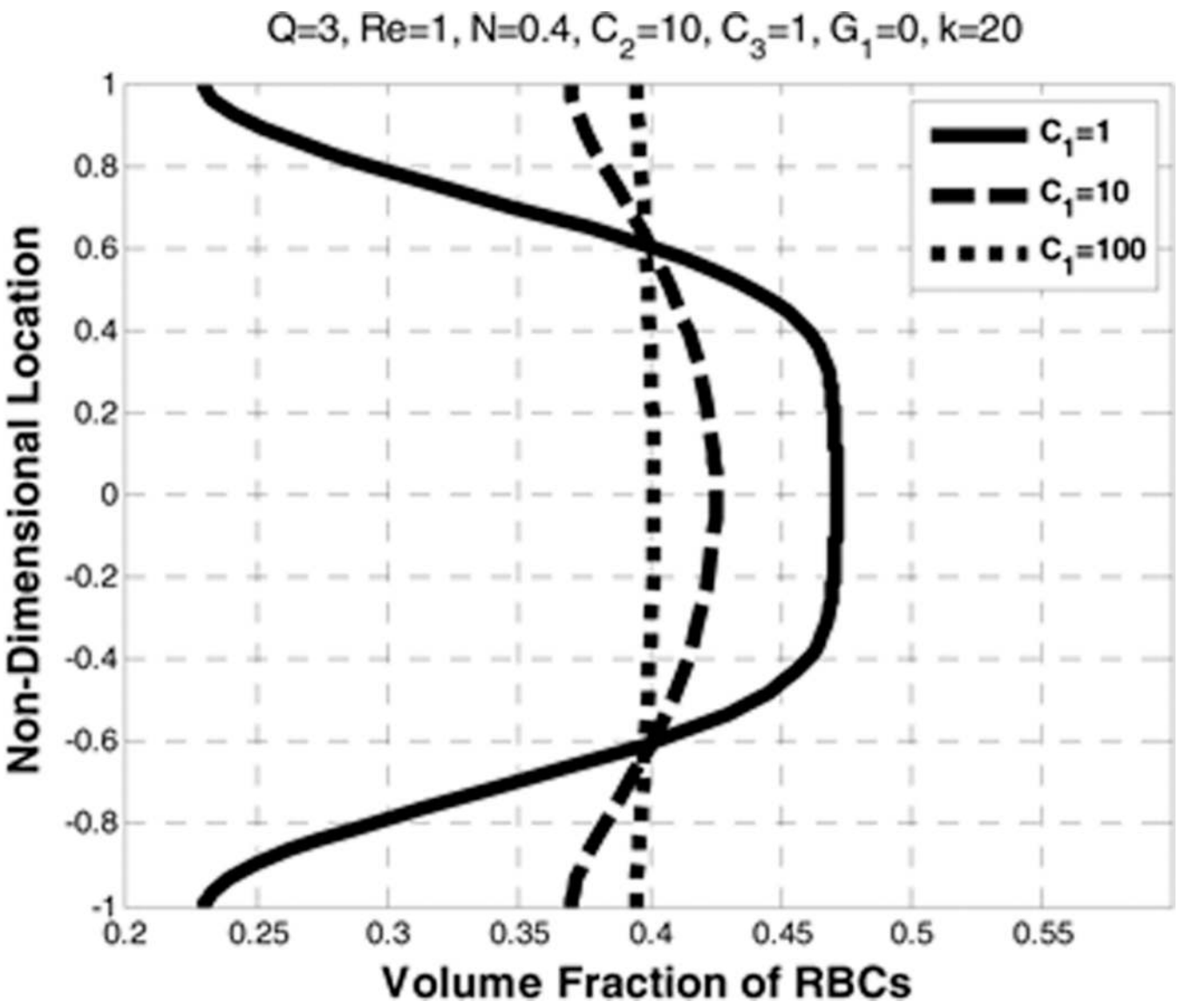

Figure 17.
Effect of density gradient coefficient (C_1) on the volume fraction of RBCs

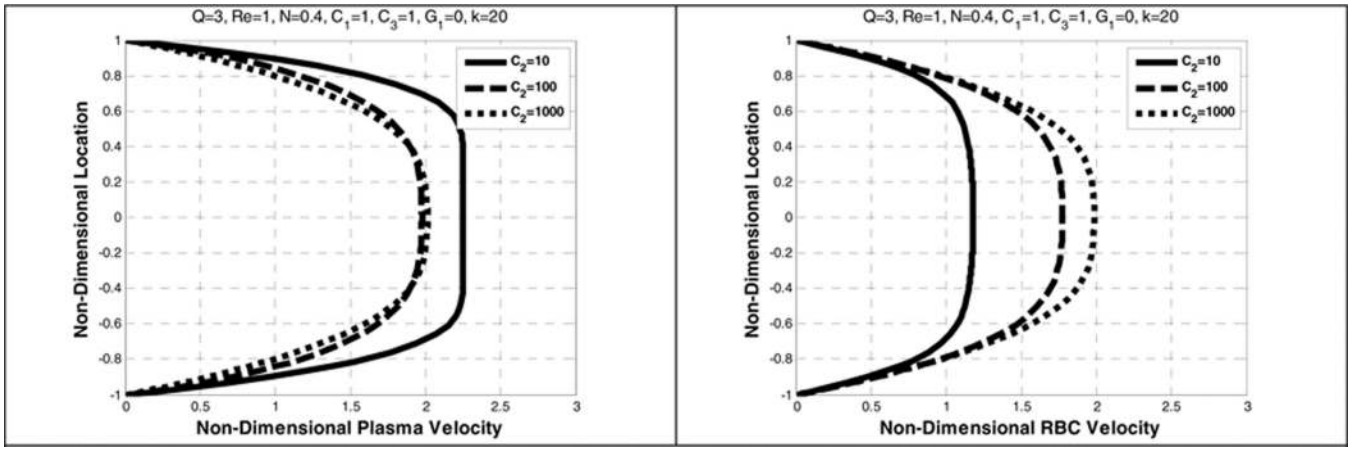

Figure 18.
Effect of drag coefficient (C_2) on the plasma velocity (left) and the RBC velocity (right)

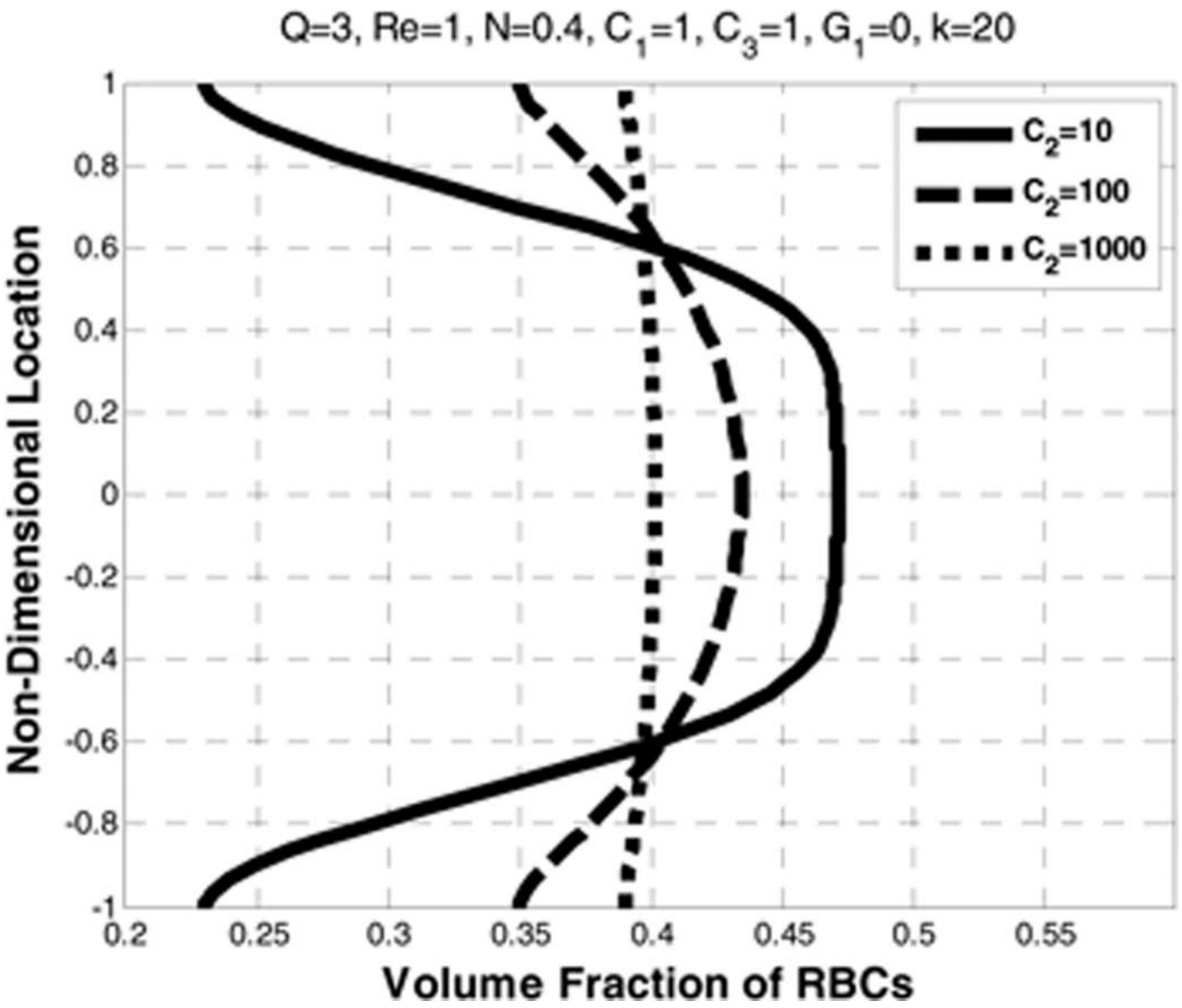

Figure 19.
Effect of drag coefficient (C_2) on the volume fraction of RBCs

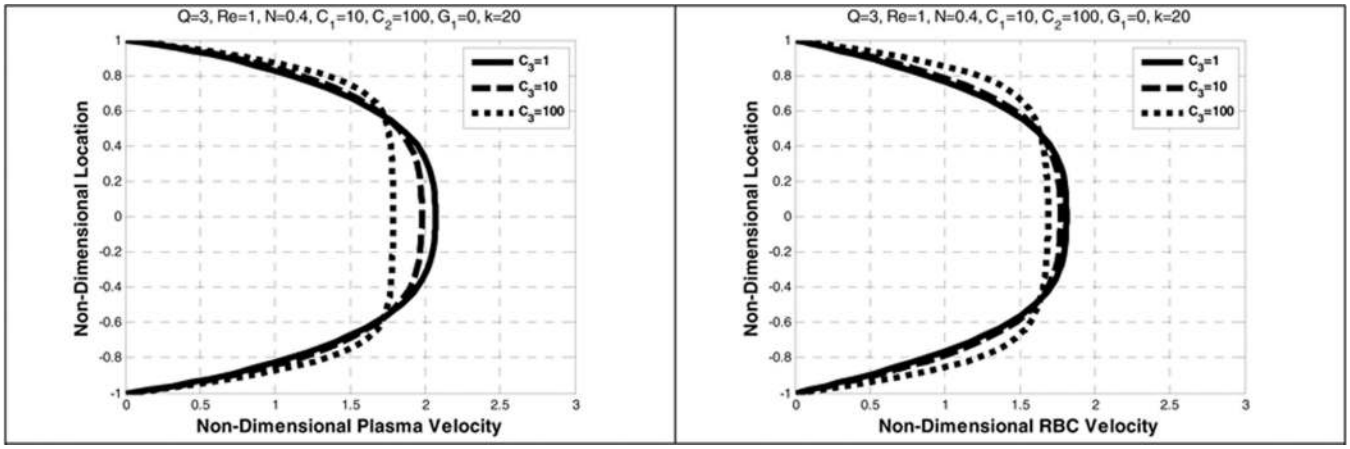

Figure 20.
Effect of lift coefficient (C_3) on the plasma velocity (left) and the RBC velocity (right)

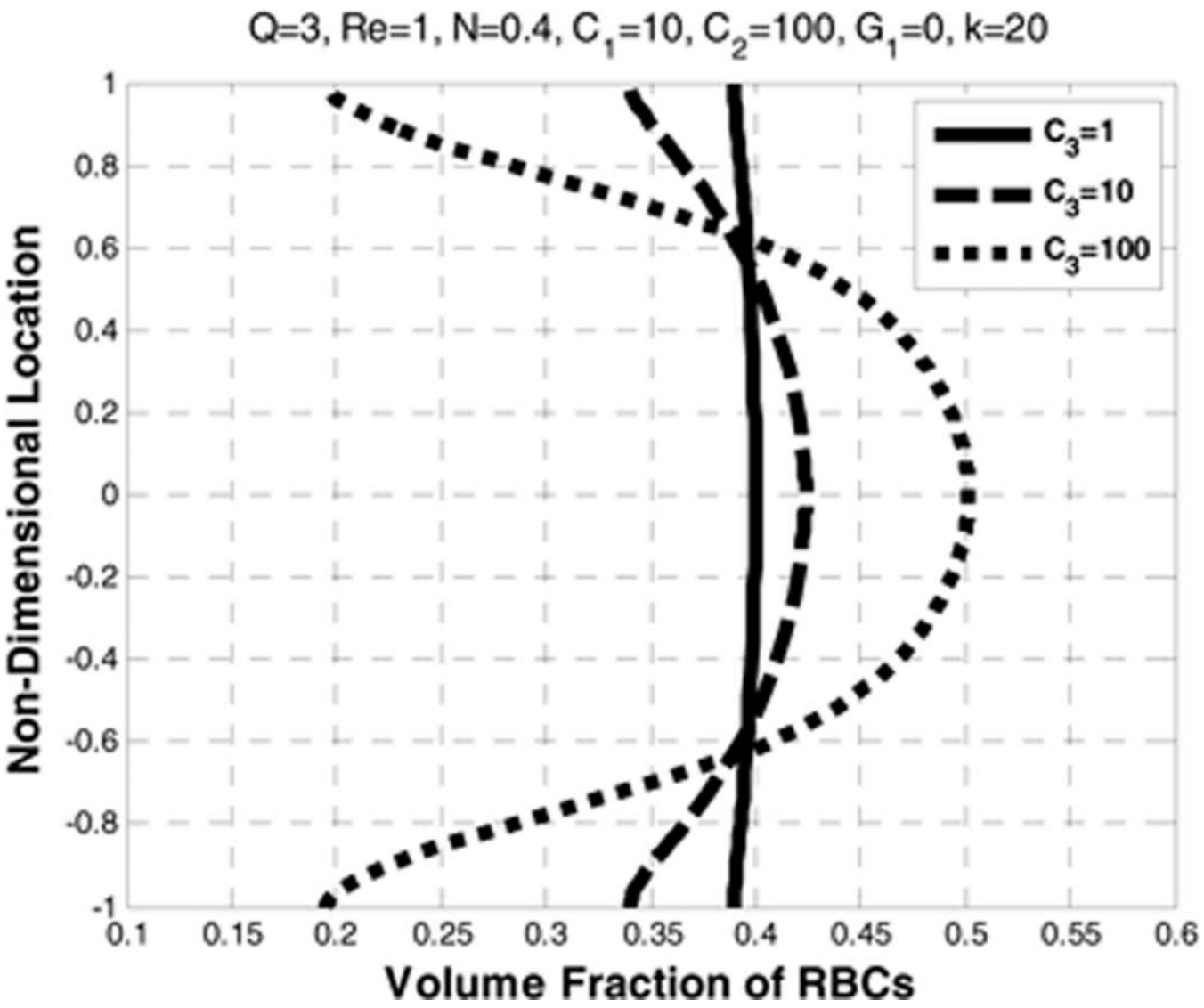

Figure 21.
Effect of lift coefficient (C_3) on the volume fraction of RBCs

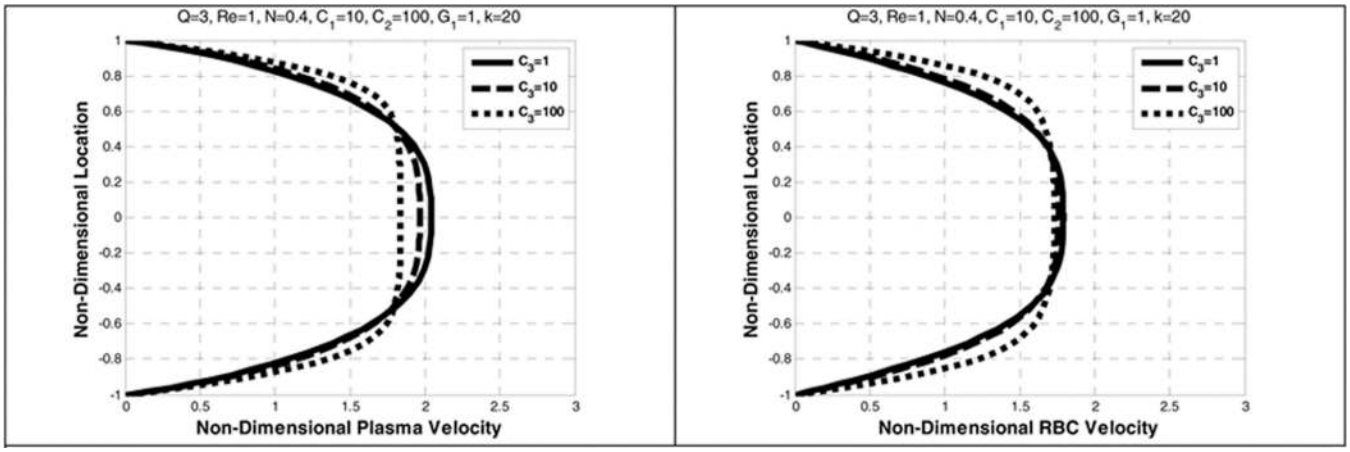

Figure 22.
Effect of lift coefficient (C_3) on the plasma velocity (left) and the RBC velocity (right)

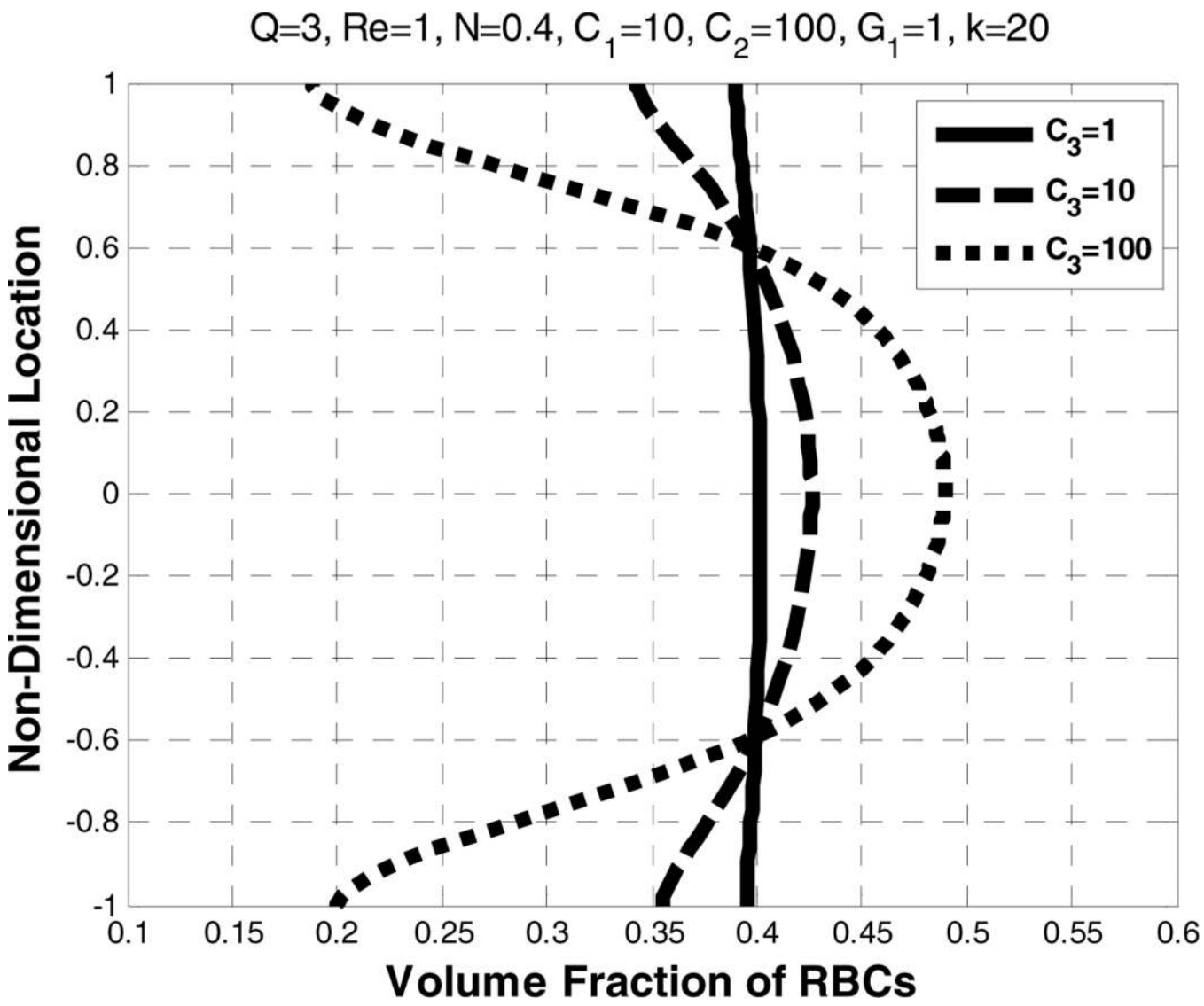

Figure 23.
Effect of lift coefficient (C_3) on the volume fraction of RBCs

Table 1

Re	0.1, 1, 100, 1000
N	0.1, 0.4, 0.7
C_1	1, 10, 100
C_2	10, 100, 1000
C_3	1, 10, 100
G_1	0.1, 1, 10
B_{31}	10, 50, 100
B_{32}	100, 200, 500
κ	0, 0.1 20, 60, 100, 1000
Q	

Table 2

Flow rates (Q) for plasma and RBC components

Reynolds number	**0.1**	**1**	**100**
Q_{plasma}	2.0	2.2	2.5
Q_{RBC}	1.0	0.8	0.5
Q_{total}	3.0	3.0	3.0
Q_{slip}	1.0 (33%)	1.4 (47%)	2.0 (66%)